

STRUCTURE AND THERMODYNAMICS OF METAL
TRIIODIDES IN SOLUTION

By

JOHN DAVID MILLER

⁴
Bachelor of Science
Southeast Missouri State University
Cape Girardeau, Missouri
1968

Master of Science
Oklahoma State University
Stillwater, Oklahoma
1972

Submitted to the Faculty of the Graduate College
of the Oklahoma State University
in partial fulfillment of the requirements
for the Degree of
DOCTOR OF PHILOSOPHY
May, 1973

Thesis

1973B

17648s

cop 2

FEB 15 1974

STRUCTURE AND THERMODYNAMICS OF METAL
TRIIODIDES IN SOLUTION

Thesis Approved:

Will Purdie

Thesis Adviser

J. Paul Alford

Tom E. Moore

H. Chris Spivey

D. D. Durham

Dean of the Graduate College

873329

ACKNOWLEDGMENTS

I wish to express my gratitude to Dr. Neil Purdie for his patience, guidance, and understanding throughout this study, and for his assistance in the preparation of this thesis manuscript. Further appreciation is expressed to Dr. Paul Devlin for his invaluable assistance in obtaining and interpreting the Raman spectra. I also wish to thank other members of the faculty and my fellow students for their assistance and encouragement.

TABLE OF CONTENTS

Chapter	Page
I. INTRODUCTION.	1
Historical	1
Statement of the Problem	5
II. TECHNIQUES.	6
Raman Spectra.	6
U. V.-Visible Spectra.	12
Methods for Multi-Species,	12
III. IONIC INTERACTIONS IN ELECTROLYTE SOLUTIONS	16
Introduction	16
The Structure of Water	16
Ion Association.	17
Thermodynamics of Ion-Pair Formation	20
IV. EXPERIMENTAL RESULTS AND TREATMENT OF THE DATA.	22
Solutions and Chemical Under Study	22
Raman Spectra of KI_3	23
Raman Spectra of TlI_3	29
U.V.-Visible Spectral Data for KI_3	29
U.V.-Visible Spectral Data of TlI_3	36
Spectral Data in CH_3CN	42
V. KINETIC STUDY	48
VI. DISCUSSION.	50
Introduction	50
Raman Spectra,	50
U.V.-Visible Spectra	52
VII. SUGGESTIONS FOR FUTURE WORK	56
A SELECTED BIBLIOGRAPHY	57

LIST OF TABLES

Table	Page
I. Thermodynamic Properties of I_5^- at 25°C	4
II. Thermodynamic Properties of I_6^{-2} at 25°C.	4
III. Raman and I.R. Active Modes for a Triatomic Molecule. . .	11
IV. U.V.-Visible Data at Maximum Absorption of KI_3 at 5°C in H_2O	32
V. U.V.-Visible Data at Maximum Absorption of KI_3 at 25°C in H_2O	33
VI. U.V.-Visible Data at Maximum Absorption of KI_3 at 45°C in H_2O	34
VII. Extinction Coefficients and Equilibrium Constants for I_3^- Formation in H_2O	37
VIII. U.V.-Visible Data at Maximum Absorption of TlI_3 at 5°C in H_2O	38
IX. U.V.-Visible Data at Maximum Absorption of TlI_3 at 25°C in H_2O	39
X. U.V.-Visible Data at Maximum Absorption of TlI_3 at 45°C in H_2O	43
XI. Association Constant of $Tl^+ + 2I_3^- = Tl(I_3)_2^-$ in 10^{-2} M Aqueous $HClO_4$	45
XII. U.V.-Visible Data at Maximum Absorption of KI_3 at 25°C in CH_3CH	46
XIII. Equilibrium Constants for I_3^- Formation in CH_3CN	47
XIV. Comparison of Equilibrium Constants of I_3^- Formation at 25°C in H_2O	52
XV. Comparison of ΔG° , ΔH° , and ΔS° for I_3^- Formation at 25°C, in H_2O	53
XVI. Comparison of Thermodynamic Properties.	54

LIST OF FIGURES

Figure	Page
1. Schematic of Raman Apparatus,	10
2. Raman Spectra of $KI/I_2 = 1$ in H_2O	25
3. Raman Spectra of KI_3 in Formamide	26
4. Raman Spectra of $KI/I_2 = 1$ in Dioxane-Water, 16:1	27
5. Raman Spectra of $KI/I_2 = 50/1$ in H_2O	28
6. Raman Spectra of $Tl(I_3)_2^-$ in H_2O	30
7. Plot of Log K Vs. $1/T$ for KI_3 in H_2O	35
8. U.V.-Visible Spectra of KI_3 and TlI_3 in H_2O	40
9. Plot of Log K Vs. $1/T$ for $Tl(I_3)_2^-$ in H_2O	44

GLOSSARY OF SELECTED SYMBOLS

a_i	Activity
σ_a	Distance of Closest Approach
A	A Constant of the Debye-Hückel Equation
\AA	Angstrom
B	A Constant of the Debye-Hückel Equation
c_i	Analytical Concentration
D	Dielectric Constant
e.u.	Entropy Units, cal/mole $^{\circ}\text{K}$
f	Activity Coefficient
G	Gibbs Free Energy
H	Enthalpy
I	Ionic Strength
K_i	Equilibrium Constant
M	Concentration in Moles per Liter
nm	Nanometer
OD	Optical Density
p	Depolarization Ratio
R	Gas Law Constant
S	Entropy
T	Absolute Temperature
V_i	Normal Vibration Mode
α	Polarizability
β	Stability Constant

GLOSSARY OF SELECTED SYMBOLS (Continued)

Δ	Change in
ϵ	Extinction Coefficient
μ	Chemical Potential
[]	Concentration

CHAPTER I

INTRODUCTION

Historical

It has been recognized since the early days of modern chemistry that halide ions have the ability to associate with halogen or inter-halogen molecules to form polyhalide ionic complexes (1). For example, shortly after the discovery of iodine it became apparent that its solubility in water and other solvents was greatly increased by the addition of potassium iodide. The reason for this was debated for sometime, and the formation of a triiodide ion was not readily accepted. In 1877 Johnson (2) isolated some large blue crystals which he claimed were potassium triiodide. A later synthesis showed that this compound was simply a mixture of potassium iodide and iodine (3). Although the simple metal trihalides have now been known for about 100 years, the nature of the bonding of these compounds is still imperfectly understood. In spite of the large volume of literature on polyhalide complexes, both the data and conclusions are at times contradictory (4,5,6).

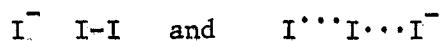
The reaction of iodine with iodide ion, $I_2 + I^- = I_3^-$, has been the one polyhalogen equilibrium most frequently studied. There remains considerable debate concerning both the structure and the thermodynamic properties of the triiodide ion (4-13). There are experimental reasons to believe that in the solid phase, and in some cases in solution, the triiodide ion is distorted from $D_{\infty h}$ symmetry. X-ray, Mossbauer, and pure

quadrupole resonance studies of CsI_3 have shown that the triiodide ion is not linear centrosymmetric (14-16). On the other hand with large soft cations the triiodide ion appears to be centrosymmetric (13). In the solid phase it is feasible to conclude that the distortion is caused either by crystal structure or by cation interaction (17). In solution this distortion can be caused by either one of two factors; solvent interaction or ion-pair formation with a suitable cation.

Several Raman and I.R. studies of the triiodide ion in solution have been done in the past, but conclusions from the results have been contradictory (5,6,7). In 1965 Ginn and Wood (6) reported the results of a low-frequency infrared study of Bu_4NI_3 in various solvents and a nujol null. All of these systems showed a strong band between $133\text{-}140\text{ cm}^{-1}$, and no band at $109\text{-}113\text{ cm}^{-1}$ which according to Person et al. (18) should be the position of the only Raman band due to the triiodide ion. This data supports the linear centrosymmetric $D_{\infty h}$ structure. Hayward and Hendra (4) in 1966 reported that they were unable to obtain the laser Raman spectra of the triiodides due to the intense color of the media. Their far infrared data on the other hand agrees closely with those of Ginn and Wood (6). Maki and Forneris (5) in the same year reported Raman spectra of triiodides using a rubidium excitation unit (19). Two features of these spectra were bands at 112 and 145 cm^{-1} which were assigned to the V_1 and V_3 modes, results which support the arguments for a linear noncentrosymmetric structure.

As the experimental work was progressing, the nature of the bonding in the polyhalogen complexes had become the subject of much discussion among theoreticians (20). A molecular orbital description of the bonding in triiodide was provided by Pimentel (17). Although quantitative

calculations are almost meaningless due to the number of approximations, certain qualitative conclusions can be drawn. Two general characteristics of the bonding in these molecular ions are 1) the bond angles are close to 90 or 180°, and 2) the bond lengths are slightly longer than the sum of atomic covalent radii (21). Electrostatic interactions were first put forward by Van Arkel and De Boer (22) to account for the bonding in polyhalogen complexes. The bond is treated essentially as an ion-dipole interaction. Hence, the electrostatic interaction between an iodide ion and an iodine molecule will result in an asymmetrical triiodide ion, because the bonds in the triiodide are essentially nonequivalent (23). The valence bond representation of the triiodide ion is expressed in terms of resonance between the structures:



Whether an equilibrium state with equivalent or nonequivalent bonds is obtained will depend on the nature of the system. Calculations done by Slater (24) have shown that a plot of the potential energy vs atomic distance, between two of the atoms in triiodide, has two minima and that the central iodide ion could be oscillating between these two minima.

The U.V.-visible spectrum of the triiodide ion is well documented in the literature (7,25,26). The characteristics of this spectrum are two bands one centered around 350 nm and the other around 285 nm. Spectrophotometric data can be used for equilibrium studies. The equilibrium constant for the formation of the triiodide ion has been measured spectrophotometrically as well as in several other ways. The values in water at 25°C range from 709 to 780 (7). Several different techniques have also been used to measure the enthalpy of formation for the tri-

iodide ion, some of the more significant values at 25°C range from -3.6 to -5.1 kcal/mole (11).

Attempts have been made to explain the inconsistencies in the calculated formation constants and heats in the triiodide system by introducing higher order complexes, such as the dimer I_6^{-2} and the polyions formed by reaction of I_3^- with additional iodine, I_5^- and I_7^- (19,27,28). Ramette and Sandford (28) report values for the I_5^- species, Table I, and

TABLE I
THERMODYNAMIC PROPERTIES OF I_5^- AT 25°C

K_5	ΔG kcal/mole	ΔH kcal/mole	ΔS e.u.
9	-1.3	+12	50

Davies and Gwynne (27) for the I_6^- species, Table II.

TABLE II
THERMODYNAMIC PROPERTIES OF I_6^{-2} AT 25°C

K_6	ΔG kcal/mole*	ΔH kcal/mole	ΔS e.u.*
1.2	-0.11	-0.77	-2.2

*Calculated by author from reported values.

Under certain experimental conditions (e.g., aqueous solutions) polyions are unlikely possibilities and an alternative explanation is the formation of ion-pairs between the cation and I_3^- (29). If this is the case

then reevaluation of the experimental data on the triiodide system would be in order.

Statement of the Problem

It is obvious from the preceding paragraphs that a large amount of confusion exists concerning the nature of the polyhalide complexes. The content of this thesis describes the collection of new data which will be used for structure and thermodynamic interpretations on the triiodide system in particular.

The objective was to work on the premise that cation-triiodide interactions are of a significance equal to if not greater than polyion complex formations. Since triiodide would be classified as a soft ligand, to find experimental evidence for its association with K^+ would be at best marginal, K^+ has a record for being innocent of ion-pair formation. In the preliminary work K^+ was used to serve as a reference for the later work where Tl^+ was introduced. From qualitative arguments association might be favored between a soft cation and a soft ligand, since a univalent cation would obviously be preferred, Tl^+ was the immediate choice.

CHAPTER II

TECHNIQUES

Raman Spectra

The Raman effect is one example of a large class of light-scattering phenomena (30). All light-scattering phenomena have their origin in the fact that when a collimated beam of light is passed through a transparent medium it is passed through a transparent medium it is invariably attenuated by that medium. A common example of this type of phenomenon is the scattering of light by dust particles in a sunbeam. Light-scattering is most easily explained if it is assumed that the illuminating beam is highly collimated and monochromatic.

Suppose that the scattered light is passed through a spectrometer, it will be found that the bulk of the scattered light will be of the same frequency as the incident beam. However, a small portion of the scattered light will be found at frequencies above and below that of the incident beam. If the incident beam is taken as a zero point the displaced frequencies will correspond to some or all of the normal frequencies of the sample. This modulation of frequency is the Raman effect (31).

A detailed description of the Raman effect requires a knowledge of quantum theory. However, the existence of the effect is easily predicted from classical electromagnetic theory. A molecule placed in an electromagnetic field will have its charge distribution periodically disturbed.

The resulting induced dipole moment acts as a source of radiation and gives rise to the light-scattering phenomena mentioned above. This dipole moment is generally expressed as the dipole moment per unit volume, i.e., the polarization. The polarization, \bar{P} , is proportional to the inducing electromagnetic field, \bar{E} :

$$\bar{P} = \alpha \bar{E} \quad (2.1)$$

where α is the polarizability and \bar{E} is given by the expression:

$$\bar{E} = \bar{E}_0 \cos 2\pi Vt \quad (2.2)$$

On substitution the expression for the polarization becomes:

$$\bar{P} = \alpha \bar{E}_0 \cos 2\pi Vt \quad (2.3)$$

The polarizability, α , consists of two parts, α_0 which is the static polarizability, and a second term which is the sum having the periodic time dependence of the normal frequencies:

$$\alpha = \alpha_0 + \sum \alpha_N \cos 2\pi V_n t \quad (2.4)$$

Combining Equations (2.3) and (2.4) we get:

$$\bar{P} = \bar{E}_0 \alpha_0 \cos 2\pi Vt + 1/2 \bar{E}_0 \sum \alpha_N [\cos 2\pi (V-V_n) + \cos 2\pi (V+V_n)] \quad (2.5)$$

Equation (2.5) correctly predicts the major qualitative features of the Raman effect. The first term accounts for the Rayleigh scattering, which has the same frequency as the incident beam. The second term which contains the variable components of the polarizability, accounts for the frequencies $(V+V_n)$ and $(V-V_n)$, the Stokes and anti-Stokes Raman bands.

The constant α , the polarizability, is of great importance in the

theory of the Raman effect, for it is known that in general \bar{P} is not parallel to \bar{E} but depends on the symmetry of the polarizability (32). Hence, a knowledge of the polarization properties of the scattered light of the Raman bands gives information about the symmetry of the molecular vibrations. To help gain information about the symmetry of the molecular vibration a depolarization ratio, p , is defined as the ratio of the intensity of the scattered light polarized perpendicular to the xy plane of the sample I_{\perp} , to that polarized parallel to this plane, I_{\parallel} , i.e.,

$$p = I_{\perp}/I_{\parallel} \quad (2.6)$$

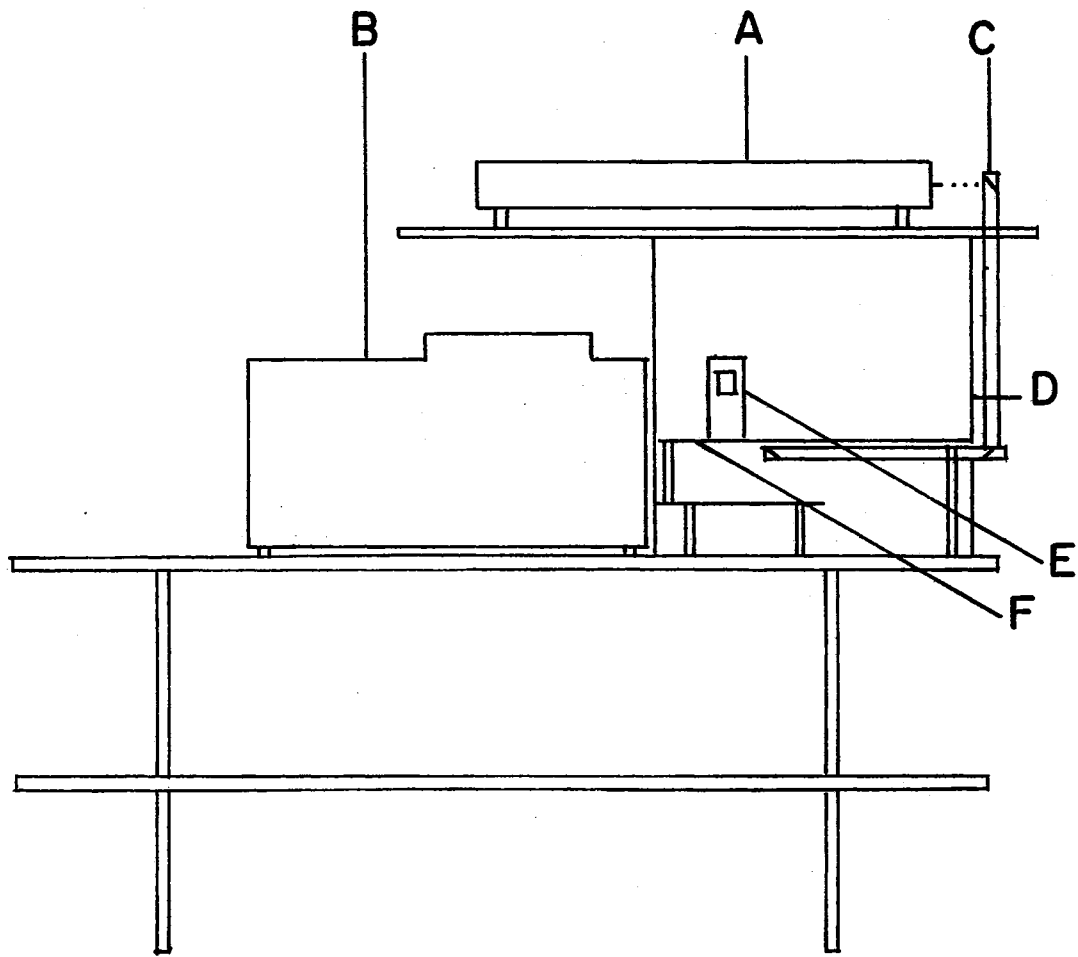
For a non totally symmetric vibration the depolarization ratio will be 6/7 or 3/4 while a symmetric vibration will have a depolarization ratio less than 6/7. As an example, p for the symmetric stretch of CCl_4 is much less than 6/7 since $I_{\perp} \approx 0$. The depolarization ratio is extremely useful in solution work in identifying the totally symmetric vibrations.

The Raman apparatus used to record the spectra was custom built from various commercial components chosen on the basis of their compatibility, reliability and cost. The monochromator unit is a pair of one-meter Czerni-Turner monochromators mechanically coupled in such a manner as to reduce stray light to a minimum. The monochromators are equipped with a cooled FW-130 photomultiplier tube. This tube has a small slit-shaped cathode as compared to the conventional tubes which have a large circular cathode. When properly cooled and aligned this tube produces a low background noise, about 2 thermal emissions/sec. A Hamner photon counting system was used for detection. Because of its ability to discriminate against pulses of improper magnitude, the photon counting system provides a high signal-to-noise ratio. The excitation source is a

Coherent Radiation Laboratories Model 52 argon ion laser. This laser provides ca. 1,000 milliwatts at $4,880 \text{ \AA}$ and $5,145 \text{ \AA}$. The laser is placed in a convenient position and the beam deflected by an appropriate lens and mirror system, as shown in Figure 1. This lens and mirror system also contains elements for polarization of the beam. The Raman scattered photons are collected by an Auto Mamiya Sekor F 1.8 camera lens and focused onto the entrance slit of the monochromator.

The particular problem of interest in this study was the triiodide ion. As mentioned in Chapter I triiodide ion solutions show a strong U. V.-visible absorption band around 350 nm. Consequently it was anticipated that these triiodide ion solutions would exhibit a resonance-enhanced Raman spectra. Preresonance Raman scattering is a process in which a sample is excited with radiation approaching an electronic absorption band of the sample (33,34). Resonance Raman spectra are characterized by high intensities and the appearance of overtones in addition to the usual fundamental frequencies. A detailed description of the resonance Raman effect is beyond the scope of this thesis.

Germane to the structural study of the triiodide ion is the identification of the I. R. and Raman active modes. To be Raman active a vibrational mode must cause a change in the polarizability, while to be I. R. active the mode must cause a change in the dipole moment. A number of structural possibilities exists for a triatomic molecule: a) linear centrosymmetric, $D_{\infty h}$, b) linear non-centrosymmetric, $C_{\infty v}$, c) non-linear symmetric, C_{2v} , and d) non-linear asymmetric, C_s . Table III list the Raman and I. R. active modes for the four possible structures (33).



A argon ion laser
B monochromator
C beam transfer optics
D enclosure
E collection lens
F optical bench

Figure 1. Schematic of Raman Apparatus

TABLE III
RAMAN AND I.R. ACTIVE MODES FOR A TRIATOMIC MOLECULE

Point Group	Raman Active	I. R. Active
$D_{\infty h}$	V_1	V_2, V_3
$C_{\infty v}$	$V_1, V_2(w), V_3(pl)$	V_1, V_2
C_{2v}	$V_1, V_2(w), V_3(ps)$	V_1, V_2, V_3
C_s	$V_1, V_2(s), V_3$	V_1, V_2, V_3

w = weak band, s = strong band, pl = large depolarization ratio, ps = small depolarization ratio.

For structures with the same number of active bands, e.g., b,c,d assignment can be made in terms of polarizability ratios. Structure determination in theory becomes a simple matter of assigning the observed vibrational modes and comparing with the predicted spectra and choosing the best correspondence (30).

In studying the structure of a molecule it would be helpful to look at the spectra of a single molecule. Since the development of the technique of matrix isolation it is possible to do this (35,36). The general technique consists of the dispersion of an active species, A, in a matrix of M, at temperatures sufficiently low to prevent diffusion of the active species A. The ratio M/A is kept high to preclude A-A interactions. In this particular study we plan to look first at I_2 trapped in H_2O matrix, pure TII, and finally I_2 trapped in a TII matrix. Hopefully some TII_3 will be formed which could become important to the interpretation of the spectra from solution in terms of intimate ion contact.

U. V.-Visible Spectra

The U. V.-visible spectrum of the triiodide solutions were recorded with a Cary recording spectrophotometer Model 14, using quartz cells with a path length of 1.00 cm.

Any spectrophotometric method is based on the Beer-Lambert law:

$$\text{Log}_{10}(I/I_0) = \text{OD} = \epsilon b C \quad (2.7)$$

I_0 and I are the intensities of the incident and transmitted radiation, OD is the optical density, ϵ is the molar extinction coefficient at a particular wave length, b the light path length in cm, and C is the concentration of the solution. For a solution which contains only one absorbing species a plot of optical density vs. concentration will be a straight line with slope equal to ϵ . If a plot of optical density vs. concentration is not a straight line this is a good indication that more than one species is absorbing.

Methods for Multi-Species

Consider a solution containing the species M and X which participate in the following equilibrium reaction:



The optical density for a one cm light path is given by:

$$\text{OD} = \epsilon_M [M] + \epsilon_X [X] + \epsilon_{MX} [MX] \quad (2.9)$$

or

$$\text{OD} = \epsilon_M (a-x) + \epsilon_X (b-x) + \epsilon_{MX} x \quad (2.10)$$

where a and b are the total molarity of M and X respectively and x is the concentration of the complex MX . If it is possible to find a wavelength where only the new species absorbs Equation (2.10) reduces to:

$$OD = \epsilon_{MX}x \quad (2.11)$$

Equation (2.11) can be combined with the equation for the thermodynamic association constant,

$$K = \frac{xf_{MX}}{(a-x)(b-x)f_M f_X} \quad (2.12)$$

where f 's are the respective activity coefficients, to give the following relationship for the absorption of only MX :

$$1/K\epsilon_{MX} = \frac{[b(a-x)f_M f_X]/[ODf_{MX}] - [(a-x)f_M f_X]/\epsilon_{MX}f_{MX}}{f_{MX}} \quad (2.13)$$

If the activity coefficients are assumed to be constant a plot of $b(a-x)/OD$ vs. $(a-x)$ will have slope $1/\epsilon_{MX}$ and intercept $1/K\epsilon_{MX}$. These values can then be inserted into Equation (2.13) to obtain a first value of x . This value can then be used to obtain a new value of ϵ_{MX} and K and so on, until successively consistent values are obtained (37). In practice it is uncommon to find spectra so simple that X and MX absorb at distinctly different wavelengths.

Another method of treating spectrophotometric measurements of the formation of complexes in solution is the method of continuous variation first introduced by Job (38), although the principles were previously outlined by Denison (39) in 1912. If a measured experimental property is a linear function of concentration, such as optical density, and only one complex is important, the method of continuous variation is capable of yielding both the stoichiometric composition and the association con-

stant of the complex. Suppose that two reactants M and A participate in the equilibrium reaction



and that both solutions of concentration c , are mixed by the addition of Y liters of A to $(1-Y)$ liters of M so that Y is less than 1, then assuming that the volume change on mixing is negligible, and that the activity coefficients are constant, the concentration of each species is given by:

$$[M] = c(1-Y) - [MA_x] \quad (2.15)$$

$$[A] = cY - x[MA_x] \quad (2.16)$$

$$[MA_x] = \beta_x [M][A]^x \quad (2.17)$$

By differentiating Equations (2.15) to (2.17) with respect to Y , setting $d[MA_x]/dY = 0$ and eliminating $[M]$, $[A]$, and $[MA_x]$ it can be shown that the condition for a maximal $[MA_x]$ is given by:

$$\beta_x c^x [(x+1)Y_{\max} - x]^{x+1} = [x - (x+1)Y_{\max}] \quad (2.18)$$

where Y_{\max} is the value of Y for which $[MA_x]$ is a maximum, the corresponding value of x is given by:

$$x = Y_{\max} / (1 - Y_{\max}) \quad (2.19)$$

and the change in optical density ΔOD by:

$$\Delta OD = \epsilon_M [M] + \epsilon_A [A] + \epsilon_{MA_x} [MA_x] - \epsilon_M c(1-Y) - \epsilon_A cY \quad (2.20)$$

assuming a one cm light path. It can be shown further that by differentiating Equation (2.20), ΔOD is a maximum when $[MA_x]$ is a maximum if

$\epsilon_{MA_x} > \epsilon_M$, or a minimum if $\epsilon_{MA_x} < \epsilon_M$. Hence, the value of x corresponding to a maximum or minimum in Y can be obtained from a plot of ΔOD vs. Y . The corresponding value of β_x can then be calculated directly from Equation (2.18). Vosburg and Cooper (40) have extended the method to cases in which more than one complex is formed.

As was mentioned in the statement of the problem the particular system of interest is the possible interaction of triiodide anion with either K^+ or Tl^+ . The absorption band with maximum at 350 nm is assigned to the electronic transition $\sigma_u^* \leftarrow \sigma_g$ (41,42).

For the KI_3 system under the experimental conditions used, plots of OD vs. the concentration of iodine were straight lines. Hence, the interpretative method outlined on pp. 12 and 13 could be used in the determination of both ϵ_{I_3} and K_{I_3} , the association constant for triiodide formation:

$$K_{I_3} = \frac{[I_3^-]}{[I_2][I^-]} \quad (2.21)$$

On the other hand with Tl^+ as the counter ion, plots of OD vs. concentration of iodine were no longer straight lines. Using the method of continuous variations the stoichiometry of the Tl^+ -triiodide complex could be established but agreement in the calculated formation constants was unsatisfactory. This as it turns out is not an unusual result (43). A different method was eventually used to calculate formation constants but the detailed discussion is deferred until Chapter V.

CHAPTER III

IONIC INTERACTIONS IN ELECTROLYTE SOLUTIONS

Introduction

In studying solutions of electrolytes, it is often desirable to have a detailed knowledge of the species present. Classical theories of solutions regard the solvent as a mere provider of space in which the solute particles move, and interactions between solvent and solute are neglected. Modern theories of electrolyte solutions are based on a quite different model. The solution can be viewed as a disordered solid in which only short-range order persists (35,44). The solute and solvent are of equal importance and the classical view is acceptable only in the limit of extreme dilution, where the solvent molecules far outnumber the solute molecules. In order to understand the interactions between solute and solvent, it is necessary to have a knowledge of the structure of the solvent. Since this study and most work in general was done in water a knowledge of the structure of water is important.

The Structure of Water

It is well known that the H-O-H bond angle is $\sim 105^\circ$ and that the O-H distance is 0.97 \AA . Bernal and Fowler (45) showed that the structure of water could be considered to be tetrahedral. Hence, in the structure of ice, in which each molecule has four nearest neighbours, the molecules are held together by tetrahedrally directed hydrogen bonds

and the structure is an open one rather than a close-packed one.

The formation of this type of hydrogen bond in liquid water contributes to a lowering of the internal energy (35). Frank and Wen (46) have postulated that these bonds are being made and broken several at a time, hence, producing short-lived clusters. The molecules inside these clusters are extensively hydrogen-bonded. The clusters themselves, however, are surrounded by non-hydrogen-bonded molecules. These "flickering clusters" of various size and shape qualitatively account for a number of experimental results. Nemethy and Scheraga (47) give a rigorous statistical treatment to this model.

Ion Association

The Arrhenius theory of ionization postulates that: a) at infinite dilution electrolytes are completely dissociated, b) the equivalent conductance is independent of concentration, and c) the law of mass action holds for the equilibrium between the ions and undissociated molecules. It is now known that the second postulate is invalid since ion mobilities decrease with increasing concentration, due to the interaction of ions of opposite charge.

Debye and Hückel (48) developed the first statistical theory of electrolyte solutions. The ions are regarded as point charges distributed in a continuum which possesses a dielectric constant equal to the bulk dielectric constant. The theory seeks to calculate the average potential energy for a given ion in solution. For a binary electrolyte:

$$\mu = \mu^{\circ} + RT \ln m + RT \ln \gamma_{\pm} \quad (3.1)$$

where μ is the chemical potential of the solute, μ° the standard chemi-

cal potential, m is the molal concentration and γ_{\pm} is the mean molal activity coefficient introduced to account for the departure from ideal behavior. Debye and Hückel defined the activity coefficient based on a mole fraction scale as:

$$\text{Log}_{10} f = Z_+ Z_- A I^{1/2} \quad (3.2)$$

where I is the ionic strength (3.3) and A is a fundamental constant:

$$I = 1/2 \sum m_i Z_i^2 \quad (3.3)$$

Equation (3.2) works well for extremely dilute solutions. In order to extend the theory to higher concentrations a term which took into account the finite size of the ions was introduced. The resulting equation for the activity coefficient is:

$$\text{Log}_{10} f = -(AZ^2 I^{1/2}) / (1 + B a^0 I^{1/2}) \quad (3.4)$$

where B is a fundamental constant and a^0 is the distance of closest approach, a^0 is essentially an empirical fitting parameter. Davies (49) proposed a further modification of the Debye-Hückel equation suggested by Guggenheim (50) and this equation with $C = 0.3$ adequately describes 1:1 electrolytes up to an ionic strength of 0.1 M:

$$-\text{Log}_{10} f = AZ_1 Z_2 \left[(I^{1/2} / (1 + I^{1/2})) - CI \right] \quad (3.5)$$

The Debye-Hückel theory gives satisfactory results for the thermodynamic behavior of very dilute solutions. However, when the ions are close together the approximations of the Debye-Hückel theory are no longer valid. At these concentrations the electrical attraction of oppositely charged ions may be greater than the thermal energy of the sol-

vent. The result of this is the formation of a new species in solution, the ion-pair (35). Bjerrum (51) was one of the first to recognize this type of interaction. Hence, in solutions of weak electrolytes there may be in addition to free ions and some neutral molecules, the ion-pairs in which the ions may be separated by one or more solvent molecules.

For a pair of ions to be considered an ion-pair they must be close enough together to lose their thermodynamic independence. Bjerrum defined this distance, q , as the distance at which the mutual potential energy is equal to $2kT$. The distance q is given by:

$$q = \frac{z_+ z_- e^2}{2DkT} \quad (3.6)$$

where e is the electronic charge, D is the dielectric constant, and k is Boltzmann's constant. Bjerrum's model predicts greater ion-pair formation the higher the charges on the ions and the lower the dielectric constant of the solvent. This prediction is in general agreement with experimental results.

In the above models it was assumed that the ions were non-polarizable and that the solvent was a continuum. However, it is known that dielectric saturation occurs in the vicinity of ions (35). Ritson and Hasted (52) have calculated the dielectric constant of water as a function of distance from an ion. For a positive ion it is assumed that the dielectric constant in the first solvent layer is about four to five. Beyond this layer the dielectric constant rises rapidly until it reaches the bulk value at a distance of $4-5 \text{ \AA}$ from the positive ion. For a negative ions it is assumed that the bulk dielectric constant can be used at all distances. It has been shown that the calculated ϵ^0 values have a small dependence on the exact dielectric constant. Hence, modern

theories of dielectric saturation do not greatly improve the results from the continuum model.

An examination of simple electrostatic theory indicates the unlikelihood of the interaction of two ions of similar charge type, especially in a solvent like water which has a high dielectric constant. Hence, the interaction of two triiodides ions, in water to form I_6^{-2} is unlikely. On the other hand, the interaction of triiodide with K^+ is likely since K^+ is known to form ion-pairs with other "soft" ions. Several examples of this are K^+ interaction with $Fe(CN)_6^{-3}$, $P_3O_{10}^{-5}$, and SO_4^{-2} . The pK's for these ion-pairs are 1.3, 2.7, and 0.9 respectively (49). Since part of this study was to examine the interaction of K^+ with triiodide ion several nonaqueous solutions with D greater than and less than water, were studied. According to Bjerrum's model, Equation (3.6), the lower the dielectric constant the greater the amount of ion-pairing.

Thermodynamics of Ion-Pair Formation

For a given temperature and pressure the thermodynamic association constant, K, for the system:



is defined by:

$$K = \frac{a_{ML_n}}{a_M a_L^n} \quad (3.8)$$

where a_X is the activity of X, for simplicity the charges have been omitted. The activity is defined as the concentration of X times the activity coefficient f_X . Activity coefficients are usually calculated using some form of the Debye-Hückel equation and most commonly the ex-

tended form given by Davies (49), Equation (3.5).

Once the association constant for the reaction is known the free energy, ΔG_i° , can be calculated (53):

$$\Delta G_i^{\circ} = -RT \ln K_i \quad (3.9)$$

Physical interpretations of the equilibria based on only G° are limited since changes in ΔG_i° can be regarded as a consequence of changes in the heat and entropy of the system. For example a number of reactions with identical ΔG° values frequently turn out to have quite different enthalpies and entropies which by self-compensation leave ΔG° constant. More information is contained in the separable values of ΔH° and ΔS° and more emphasis is currently being given to accurate heat measurements. The best determination of H° is by direct calorimetry. Work of this nature is in progress in this laboratory for I_3^- . In this research $4H^{\circ}$ was determined from the temperature dependence of the association constant (53):

$$\ln (K_2/K_1) = \Delta H_i^{\circ}/R(1/T_1 - 1/T_2) \quad (3.10)$$

Once ΔG_i° and ΔH_i° are known ΔS_i° can be calculated from the Gibbs free energy equation (53):

$$\Delta G_i^{\circ} = \Delta H_i^{\circ} - T\Delta S_i^{\circ} \quad (3.11)$$

ΔH_i° is the property which is most directly related to changes in bonding, while ΔS_i° is a measure of the change of randomness and solvation.

CHAPTER IV

EXPERIMENTAL RESULTS AND TREATMENT OF THE DATA

Solutions and Chemicals Under Study

The aqueous solutions under study were prepared in 0.01 M HClO_4 and degassed with nitrogen. The HClO_4 was added to suppress hydrolysis of iodine. All solutions were stored in an ice box at 4°C until ready for use. New solutions were prepared every two weeks. The acetonitrile solutions were prepared using solvent which had been dried by storing over 4 Å molecular sieve for a minimum of 72 hours before use.

The deionized water used in all experiments was prepared by passing distilled water through a 6 ft. column of reagent grade Rexyn # 300 (H-OH) mixed bed resin (Fisher Scientific Co.). Before entering the two twelve liter storage flask, which were vented to the atmosphere through ascarite (8-20 mesh, Arthur H. Thomas Co.) to exclude CO_2 , the water was passed over a 3 ft. column of activated charcoal to remove dissolved trace organics leached from the exchange resin. Water not treated in this manner had a high fluorescence, which made it impossible to obtain Raman spectra.

The KI used in the preparation of KI_3 was Baker Analyzed Reagent with less than 0.05% chloride and bromide present. The salt was dried in a 110°C oven. Fisher Scientific Co. U. S. P. iodine was doubly sublimed before use. For the first sublimation KI was added to help remove any chloride or bromide. The iodine was stored in a sealed container.

Thallium nitrate used in the preparation of the aqueous TlI_3 solutions was obtained from the Fisher Scientific Co. lot no. 701884, and was dried in a $110^\circ C$ oven. $TlClO_4$ prepared by reacting $TlOH$ and $HClO_4$ was used in the preparation of TlI_3 for the acetonitrile solutions. Alfa Inorganics lot no. 071972 $TlOH$ and Baker Analyzed Reagent 70% $HClO_4$ were used. The concentration of the $HClO_4$ solutions was checked by titration with standardized KOH . Acetonitrile and Dioxane were also Baker Analyzed Reagent grade. The tetramethyl ammonium iodide used was Eastman yellow label quality.

The temperature of the solutions used in the U. V.-visible experiments was controlled to within $0.1^\circ C$ with a Braun Thermomix II Circulator-Heater. As suggested by Davies and Prue (53) the cells were filled and emptied without removal from the cell holder. This is done in order to prevent contamination of the solutions or the cell faces. No attempt was made to control the temperature of the solutions used in the Raman study.

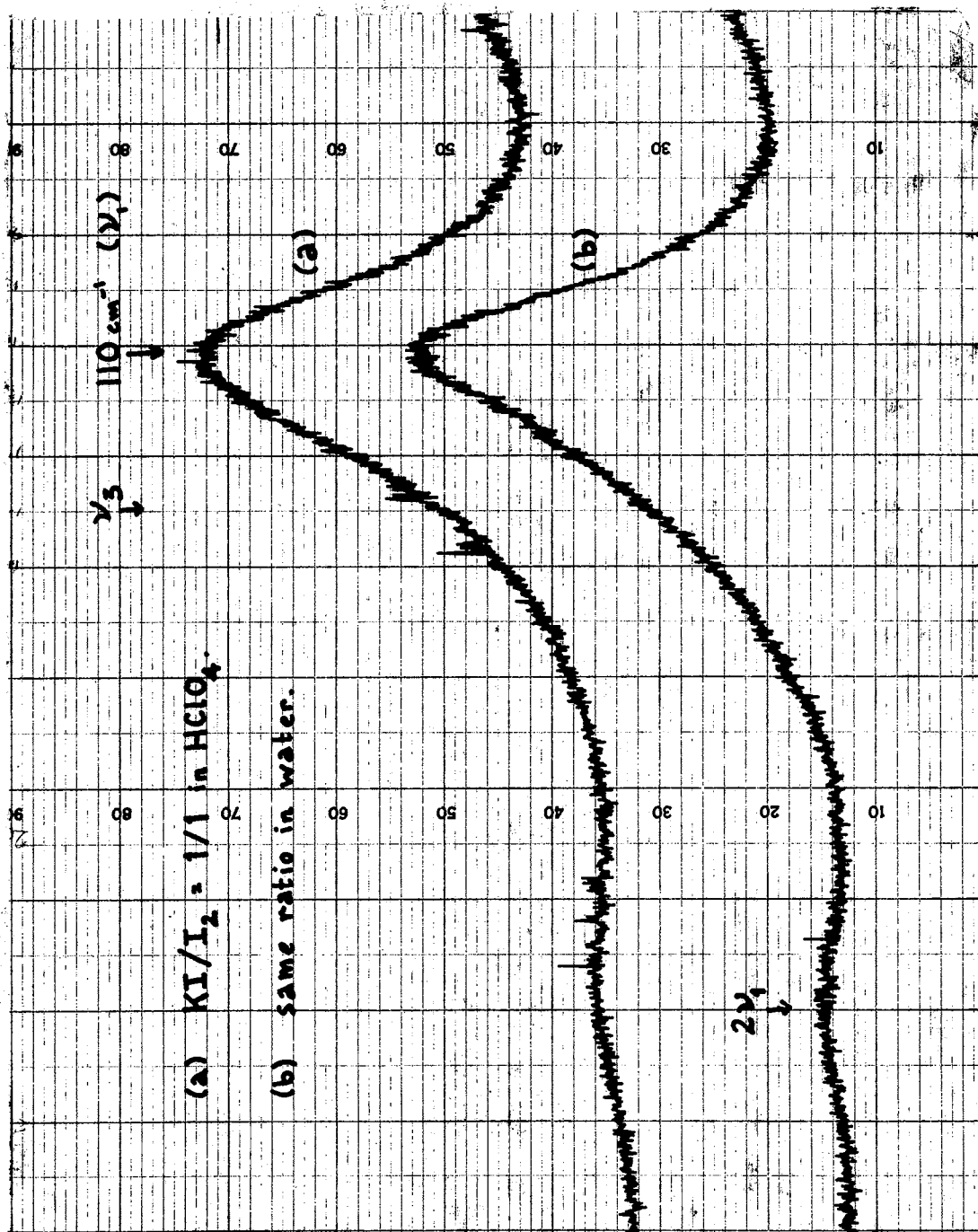
Raman Spectra of KI_3

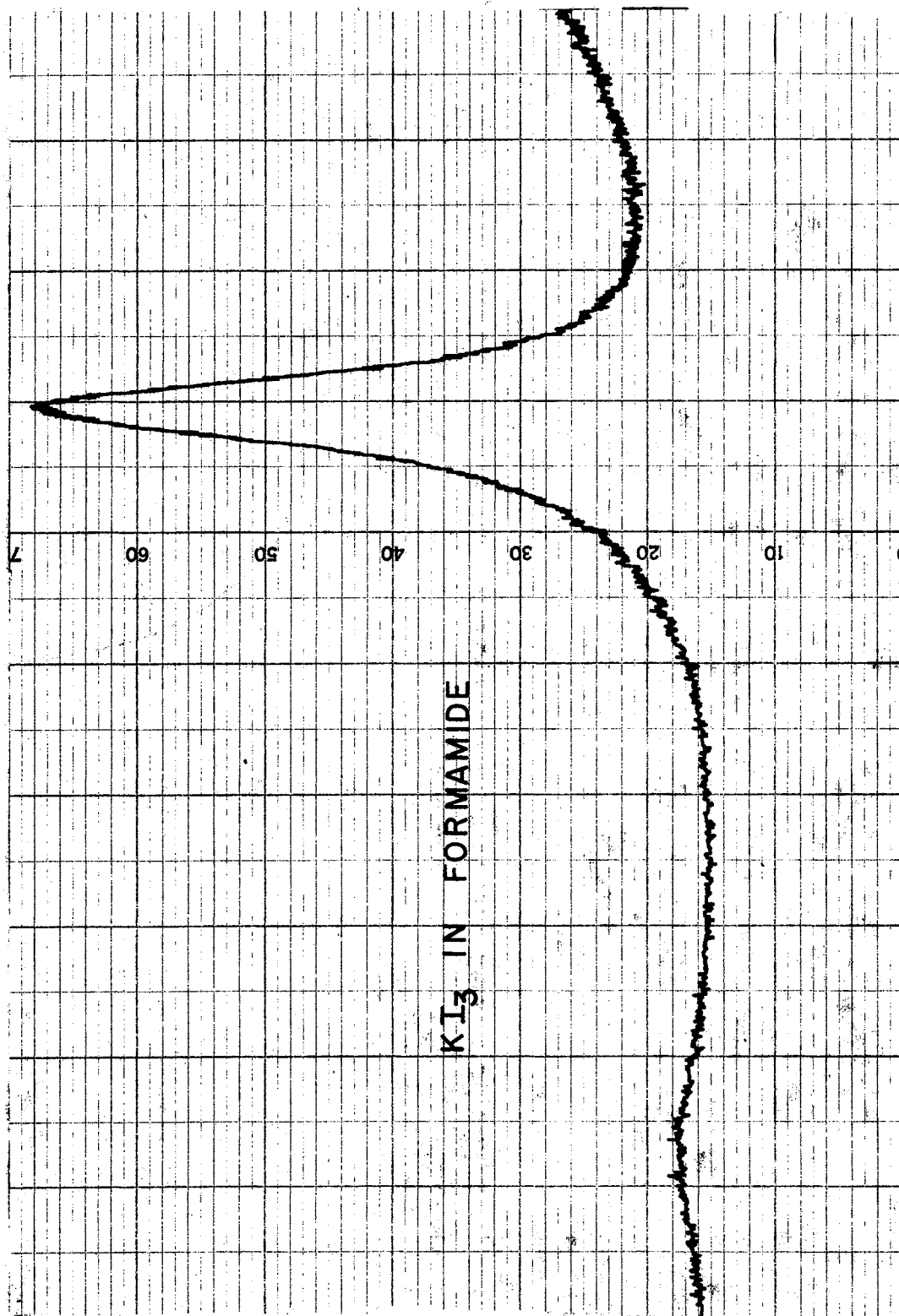
The Raman spectra were taken from 50 cm^{-1} to 300 cm^{-1} with a scanning speed of $10\text{ cm}^{-1}/\text{min.}$, using the $4,800\text{ \AA}$ excitation line of the argon ion laser. The spectra were always taken with the laser beam polarized parallel to the xy plane of the sample and again with the beam polarized perpendicular to the xy plane. As has been mentioned before the KI_3 system has two Raman bands. The relative intensities of these bands were followed as a function of concentration and dielectric constant of the medium. No attempt was made to draw any quantitative conclusions from the Raman data.

A mixture of $KI/I_2 = 1$ in water shows the typically strong V_1 band at 110 cm^{-1} , a weak V_3 band at 145 cm^{-1} , and a very weak $2 V_1$ at 220 cm^{-1} , Figure 2. However, the V_2 bending mode which should be seen somewhere between $60\text{--}80 \text{ cm}^{-1}$ was not seen due to the large liquid wing. These bands and their assignment are consistent with those reported by Maki and Forneris (5). The number of Raman active bands indicates that in this case the triiodide ion is distorted from $D_{\infty h}$ symmetry. On the other hand, a study of $(\text{CH}_3)_4\text{NI}_3$ in water and KI_3 in formamide, dielectric constant = 109, Figure 3, show one strong band around 110 cm^{-1} indicating that in these two cases the I_3^- ion is in $D_{\infty h}$ symmetry.

As the triiodide ion concentration in water is decreased it is observed that the broad V_3 shoulder decreases rapidly although it is still distinguishable at concentrations ca. 10^{-3} M . At this concentration it is reasonable to conclude that the triiodide ion distortion, evidenced by V_3 Raman activity, is solvent induced.

For a ratio of $KI/I_2 = 1$ in 16:1 dioxane-water mixtures, dielectric constant = 5, the broad V_1 band becomes much sharper and a third weak feature is developed at 165 cm^{-1} , Figure 4. Both of these effects are consistent with a strong electrostatic interaction in the lower dielectric medium. At a $KI/I_2 = 3$ ratio in the same dioxane-water mixture a moderate intensification of the 165 cm^{-1} band is observed. In this medium all three bands are distinctly separated, the original V_3 is now around 135 cm^{-1} . A gradual transition to the pure water spectrum is observed as the dioxane to water ratio is decreased. However, when KI is added in large excess over I_2 in pure water (50:1) the intensity of the 165 cm^{-1} band increases very rapidly with respect to that of V_1 , Figure 5. Similar effects were noted using LiI/I_2 in water, however, the

Figure 2. Raman Spectra of $KI/I_2 = 1$ in H_2O

Figure 3. Raman Spectra of KI_3 in Formamide

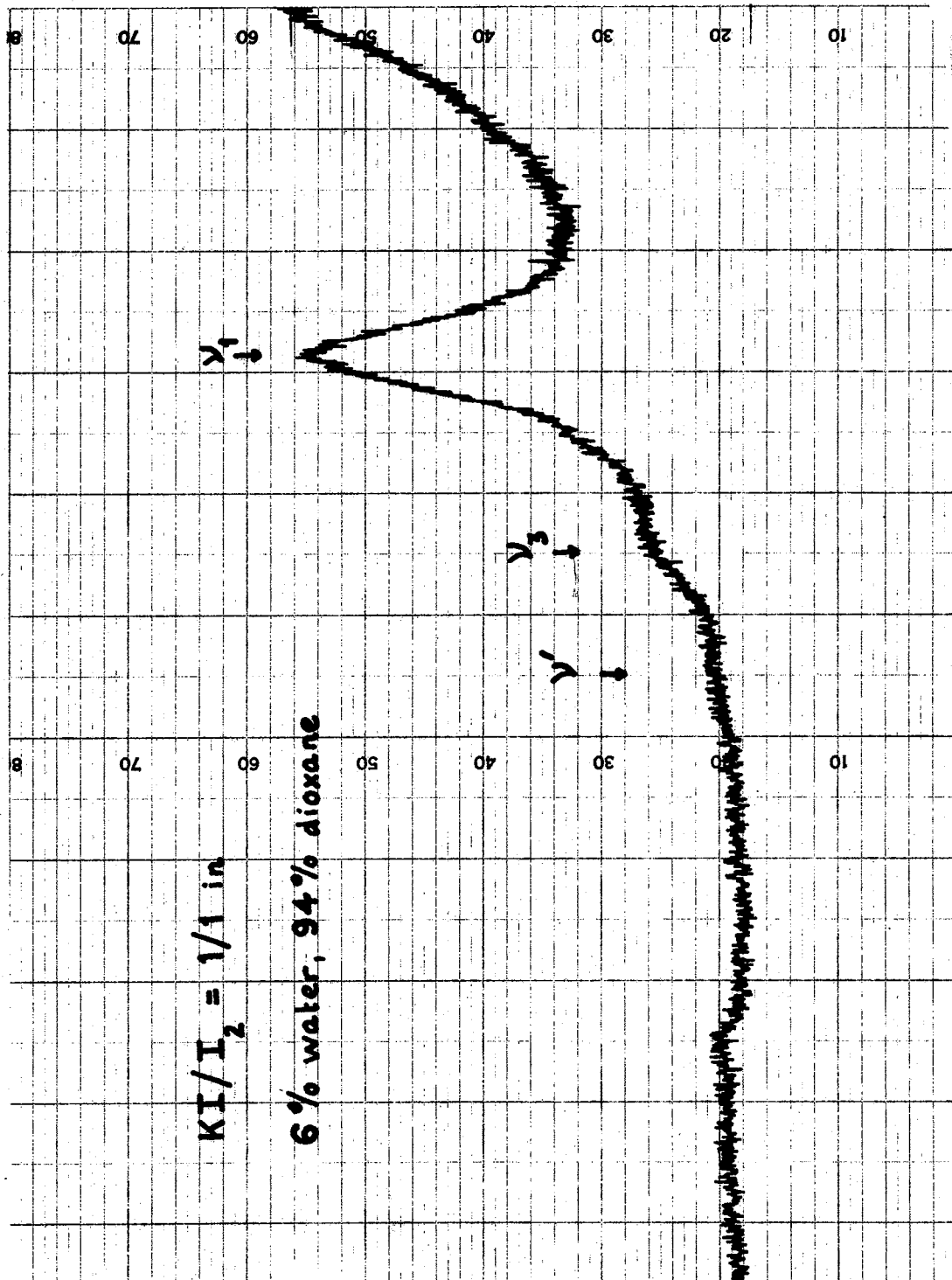


Figure 4. Raman Spectra of KI/I₂ = 1 in Dioxane-Water, 16:1

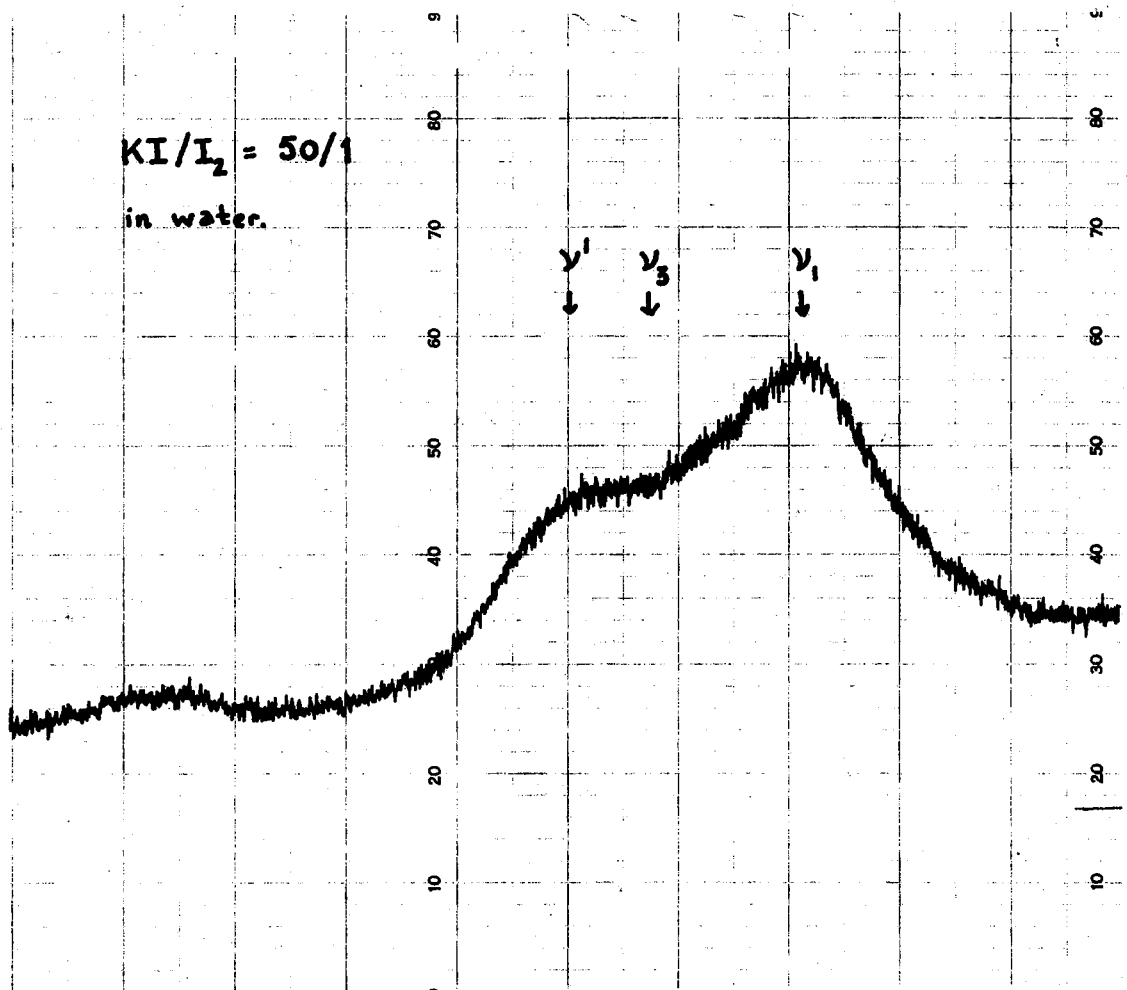


Figure 5. Raman Spectra of $KI/I_2 = 50/1$ in H_2O

association was not as great. This is as expected since Li^+ is a much smaller and harder ion than K^+ .

Raman Spectra of TlI_3

The Raman spectrum of thallium triiodide in aqueous acid shows an additional dominant feature at 130 cm^{-1} , over and above the features of the KI_3 spectra, Figure 6. This very sharp band is strongly polarized ($p = 0.2$) and is attributed to a contact ion-pair interaction which has displaced the V_1 band by 20 cm^{-1} . In spite of the very strong cation interaction the V_3 asymmetric stretch (155 cm^{-1}) remains weakly active suggesting that the intense feature at 165 cm^{-1} in very high KI/I_2 ratios is due not to intensification of V_3 but to V_1 of a new species. Equilibrium is presumed to exist between the contact and the solvent separated ion-pairs in TlI_3 since on adding dioxane the 130 cm^{-1} band becomes even sharper and more dominant as the other features decrease in intensity to a $1/20$ of that in pure water. These features are not observed in freshly prepared solutions of TlI and KI in dioxane-water or tri-n-butyl phosphate, provided oxygen is excluded. From this observation any possible complication to the spectrum from the existence of iodothallate complexes can be dismissed (55). Hence, the 130 cm^{-1} band indicates that a new species is present in solution, e.g., the ion-pair formed between Tl^+ and I_3^- which must be symmetrical because of the depolarization ratio.

U.V.-Visible Spectral Data for KI_3

The U.V.-visible spectrum of aqueous KI_3 was recorded from 400 nm to 250 nm at 5, 25, and 45°C . At each temperature the following nine

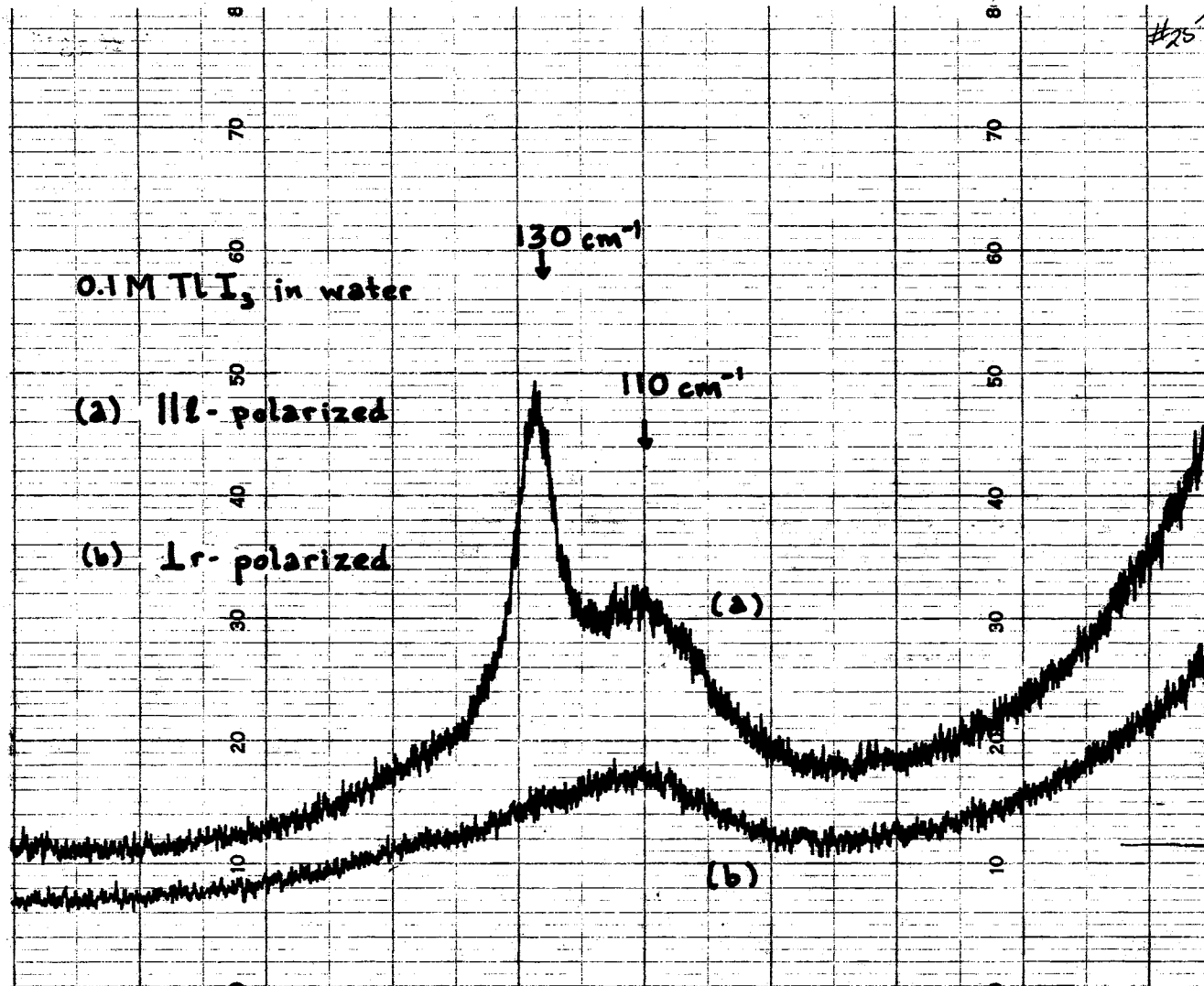


Figure 6. Raman Spectra of $Tl(I_3)_2^-$ in H_2O

ratios of the volume of I_3^- solution to total volume were used: .80, .75, .70, .65, .60, .55, .50, .45, and .40. Some examples of the absorption data at the three temperatures are shown in Tables III, IV, and V.

Since plots of the optical density vs. $[I_2]$ were linear, but did not pass through the method outlined in Chapter II, plots of $(a-x)$ vs. $b(a-x)/OD$, was used to obtain the extinction coefficients and equilibrium constants for the triiodide formation. The details of this method are as follows. First let $a = [I^-]$, $b = [I_2]$, and make an estimate as to the value of the extinction coefficient. Knowing the measured optical density and the extinction coefficient, x the amount of I_3^- , can be calculated at each data point:

$$x = [I_3^-] = OD/\epsilon_{I_3} \quad (4.1)$$

With x known a plot of $(a-x)$ vs. $b(a-x)/OD$ can be made. From this plot K_{I_3} and a new extinction coefficient can be obtained. These values are used to obtain new values of x and so on until convergence is obtained. The extinction coefficients at 370 m μ and the equilibrium constants are reported in Table VI. No correction was made for formation of a potassium triiodide ion-pair at these concentrations since from an independent study in this laboratory it has been shown that the equilibrium constant for such an ion-pair formation is around four (56).

The value of the enthalpy of formation of triiodide at 25°C can be found using Equation (3.10). This method involves plotting $\log_{10} K$ vs. $1/T$, Figure 7, and taking the slope at the point of interest. The value of ΔH° is $\Delta H^\circ = -3.80 \pm 0.20$ kcal/mole. The standard deviation of ΔH° is found on the basis of the temperature range used and the probable

TABLE IV

U.V.-VISIBLE DATA AT MAXIMUM ABSORPTION OF KI_3 AT 5°C IN H_2O

$[\text{I}^-] \times 10^4$	$[\text{I}_2] \times 10^4$	v_i/v_t	Tabulated as Optical Densities		
			295 nm	360 nm	395 nm
8.02	1.61	.80	1.89	1.20	0.52
7.52	1.51	.75	1.71	1.08	0.47
7.02	1.41	.70	1.51	0.96	0.43
6.52	1.31	.65	1.37	0.87	0.38
6.02	1.21	.60	1.24	0.79	0.33
5.52	1.11	.55	1.06	0.67	0.28
5.02	1.01	.50	0.92	0.59	0.24
4.52	0.91	.45	0.76	0.47	0.19
4.02	0.81	.40	0.59	0.37	0.16

TABLE V

U.V.-VISIBLE DATA AT MAXIMUM ABSORPTION OF KI_3 AT 25°C IN H_2O

$[\text{I}^-] \times 10^4$	$[\text{I}_2] \times 10^4$	v_1/v_t	Tabulated as Optical Densities		
			295 nm	360 nm	395 nm
8.02	1.61	.80	---	1.38	0.73
7.52	1.51	.75	1.91	1.25	0.65
7.02	1.41	.70	1.68	1.10	0.58
6.52	1.31	.65	1.46	0.96	0.52
6.02	1.21	.60	1.25	0.81	0.43
5.52	1.11	.55	1.09	0.71	0.37
5.02	1.01	.50	0.93	0.61	0.32
4.52	0.91	.45	0.76	0.50	0.27
4.02	0.81	.40	0.60	0.40	0.21

TABLE VI

U.V.-VISIBLE DATA AT MAXIMUM ABSORPTION OF KI_3 AT 45°C IN H_2O

$[\text{I}^-] \times 10^4$	$[\text{I}_2] \times 10^4$	v_i/v_t	Tabulated as Optical Densities		
			295 nm	360 nm	395 nm
8.02	1.61	.80	1.57	1.00	0.61
7.52	1.51	.75	1.41	0.88	0.53
7.02	1.41	.70	1.25	0.77	0.46
6.52	1.31	.65	1.08	0.66	0.39
6.02	1.21	.60	0.92	0.57	0.34
5.52	1.11	.55	0.76	0.48	0.28
5.02	1.01	.50	0.64	0.41	0.24
4.52	0.91	.45	0.52	0.33	0.19
4.02	0.81	.40	0.43	0.27	0.16

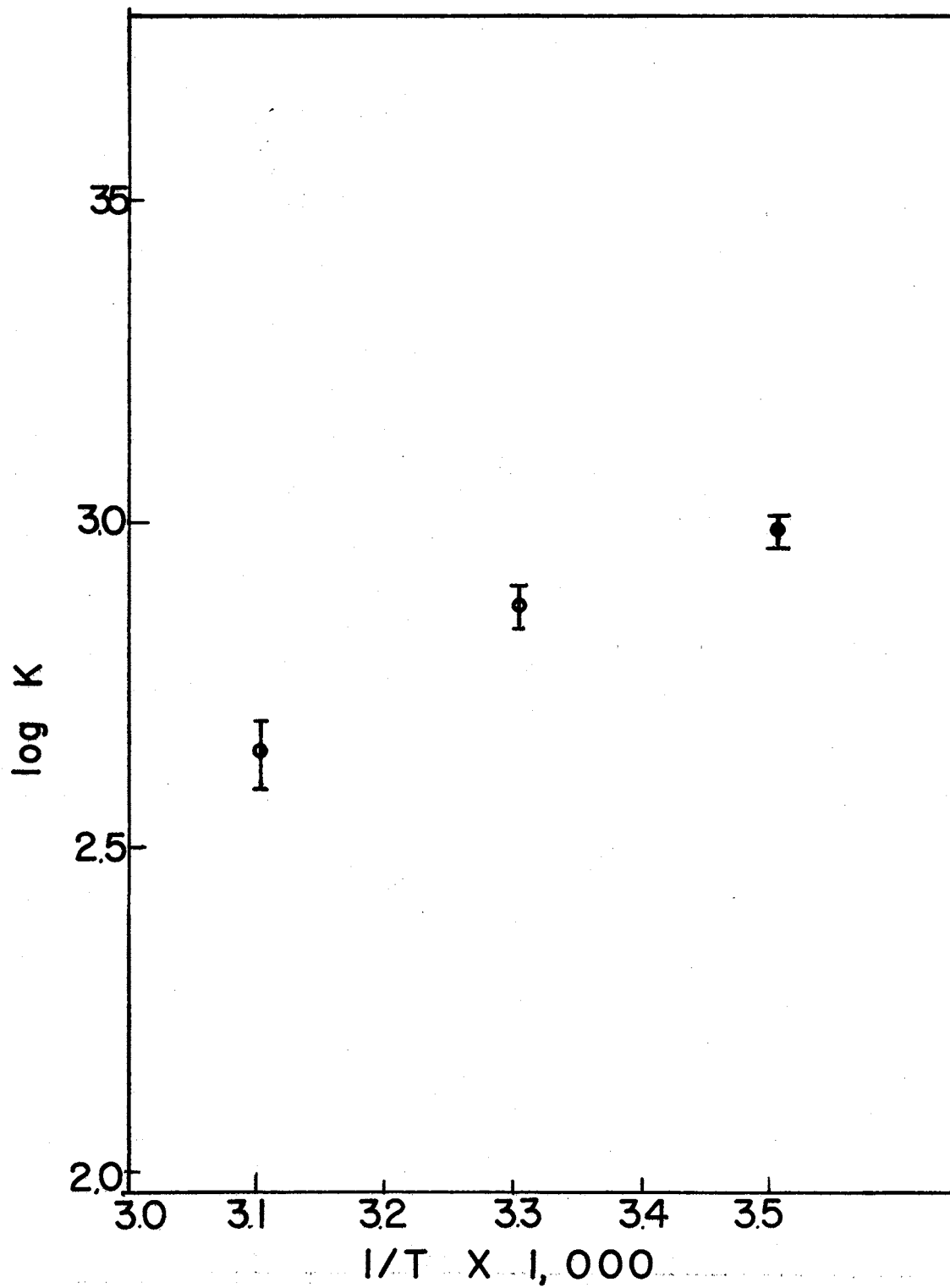


Figure 7. Plot of Log K Vs. 1/T for KI_3 in H_2O .

error in the equilibrium constant using the method outlined by King (57). The ΔG° for the reaction is about -3.90 kcal/mole which from the Gibbs free energy equation (Equation 3.11) implies that the entropy change for the reaction is near zero. This means that the reaction is enthalpy and not entropy driven.

U.V.-Visible Spectral Data of TlI_3

The spectra of the aqueous TlI_3 were also recorded from 400 nm to 250 nm at 5, 25, and 45°C. The same nine ratios as mentioned above were again used, however, instead of diluting each solution with the appropriate volume of 0.01 M $HClO_4$, the solutions were diluted with a $TlNO_3$ solution. Three different ratios of the stock concentration of Tl^+ to the stock concentration of I_3^- were used: 1:1, 1.5:1, and 2:1. Typical absorption data on the TlI_3 system are given in Tables VII, VIII, and IX.

The TlI_3 system in water was a somewhat different problem, from the fact that as the Tl^+ concentration was increased the 360 nm band shifted to 395 nm, see Figure 8. Plots of optical density vs. $[I_2]$ were not linear. Accordingly, this data could not be treated in the same manner as the KI_3 data, for there was no wavelength at which only one species was absorbing. However, if the KI_3 system is taken as a reference, plots of changes in optical density vs. the ratio of the volume of I_3^- solution to total volume (Job's treatment) can be made. These plots have a maxima at 0.67 indicating a two to one complex. The Tl^+ solutions also show an isosbestic point at 370 nm. An isosbestic point occurs if two spectra have the same optical density at a given wavelength, and if the solutions contain two absorbing species in different ratios, but the total concentration are the same in both solutions. The existence of

TABLE VII
EXTINCTION COEFFICIENTS AND EQUILIBRIUM
CONSTANTS FOR I_3^- FORMATION IN H_2O

5°C		25°C		45°C	
ϵ	K	ϵ	K	ϵ	K
1.50×10^4	$1,003 \pm 60$	1.84×10^4	760 ± 40	2.11×10^4	425 ± 35

TABLE VIII

U.V.-VISIBLE DATA AT MAXIMUM ABSORPTION OF TlI_3 AT 5°C IN H_2O

$[\text{I}^-] \times 10^4$	$[\text{I}_2] \times 10^4$	$[\text{Tl}^+] \times 10^4$	v_i/v_t	Tabulated as Optical Densities			
				295 nm	360 nm	395 nm	370 nm*
8.02	1.61	0.40	.80	1.76	0.93	0.73	1.03
7.52	1.51	0.50	.75	1.50	0.73	0.70	0.93
7.02	1.41	0.60	.70	1.23	0.54	0.65	0.84
6.52	1.31	0.70	.65	1.03	0.42	0.60	0.76
60.2	1.21	0.80	.60	0.92	0.36	0.55	0.68
5.52	1.11	0.90	.55	0.81	0.31	0.55	0.58
5.02	1.01	1.00	.50	0.68	0.25	0.43	0.51
4.52	0.91	1.10	.45	0.53	0.20	0.32	0.41
4.02	0.81	1.20	.40	0.38	0.15	0.22	0.32

*The isosbestic point.

TABLE IX

U.V.-VISIBLE DATA AT MAXIMUM ABSORPTION OF TlI_3 AT $25^\circ C$ IN H_2O

$[I^-] \times 10^4$	$[I_2] \times 10^4$	$[Tl^+] \times 10^4$	v_i/v_t	Tabulated as Optical Densities			
				295 nm	360 nm	395 nm	370 nm*
8.02	1.61	0.40	.80	----	1.26	0.86	1.07
7.52	1.51	0.50	.75	1.88	1.10	0.82	0.97
7.02	1.41	0.60	.70	1.59	0.90	0.72	0.87
6.52	1.31	0.70	.65	1.34	0.74	0.64	0.80
6.02	1.21	0.80	.60	1.29	0.71	0.61	0.70
5.52	1.11	0.90	.55	1.15	0.62	0.57	0.61
5.02	1.01	1.00	.50	1.00	0.54	0.50	0.54
4.52	0.91	1.10	.45	0.81	0.43	0.41	0.43
4.02	0.81	1.20	.40	0.65	0.35	0.34	0.35

*The isosbestic point.

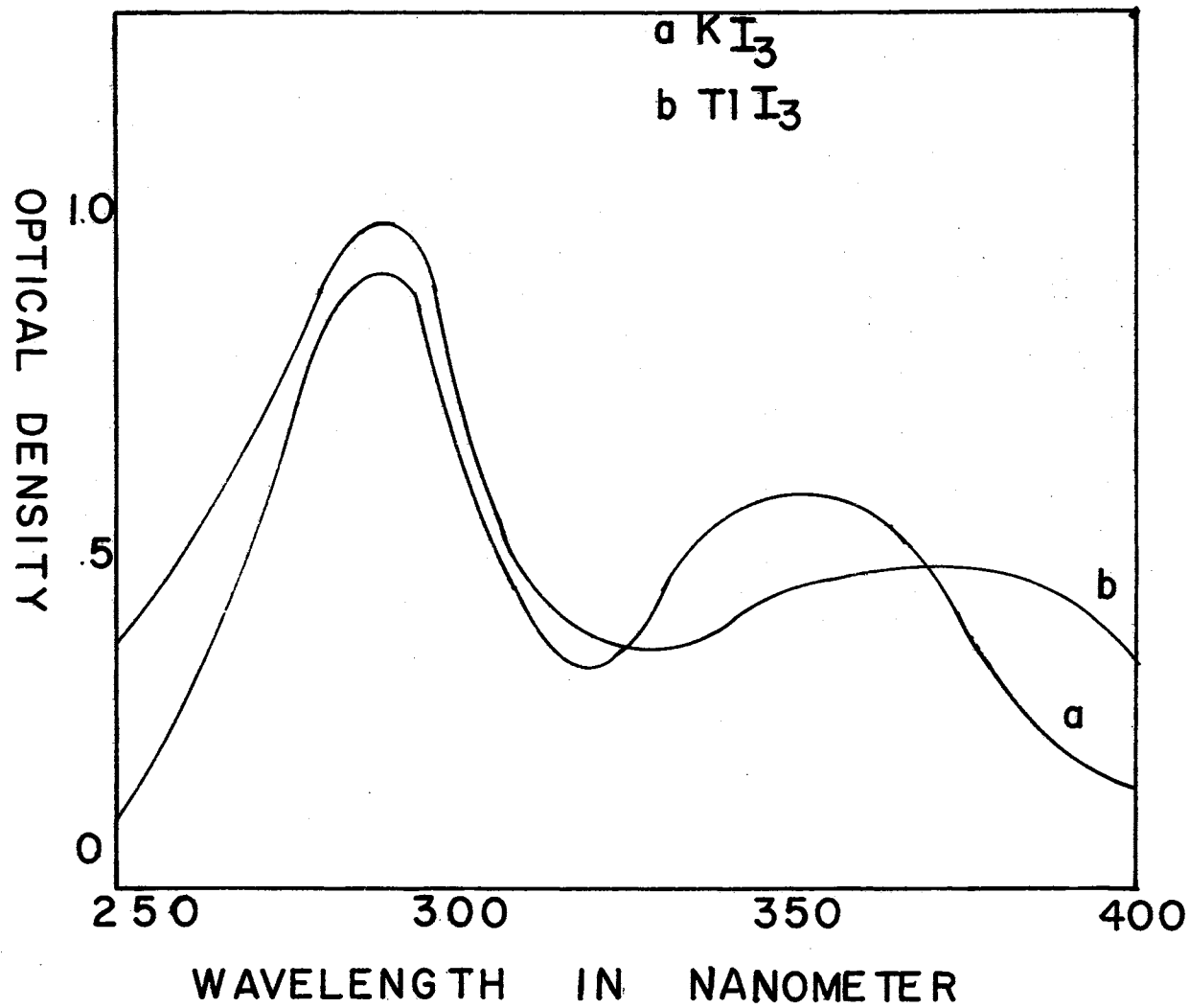


Figure 8. U.V.-Visible Spectra of KI₃ and TlI₃ in H₂O

this point reduces the number of unknowns by one, and allows the calculation of the extinction coefficient for the pure KI_3 data. Hence, an exact analytical solution for the association constant in the Tl^+ system is possible.

The association constant can be calculated from the mass balance equations:

$$C_I = [I^-] + [I_3^-] + 2[Tl(I_3)_2^-] \quad (4.2)$$

$$C_{I_2} = [I_2] + [I_3^-] + 2[Tl(I_3)_2^-] \quad (4.3)$$

$$C_{Tl} = [Tl^+] + [Tl(I_3)_2^-] \quad (4.4)$$

the equation for the optical density at the isosbestic point:

$$OD = \epsilon([I_3^-] + [Tl(I_3)_2^-]) \quad (4.5)$$

and the equations for the two association constants:

$$K_{I_3} = [I_3^-]/[I^-][I_2] \quad (4.6)$$

$$K_{Tl} = [Tl(I_3)_2^-]/[Tl^+][I_3^-]^2 \quad (4.7)$$

Letting $a = [I_3^-]$ and $b = [Tl(I_3)_2^-]$ Equation (4.5) becomes:

$$b = (OD/\epsilon) - a \quad (4.8)$$

By the appropriate combination of Equations (4.2), (4.3), and (4.8) the expression for K_{I_3} can be written as:

$$K_{I_3} = a/[(C_I - 2OD/\epsilon + a)(C_{I_2} - 2OD/\epsilon + a)] \quad (4.9)$$

Now letting $x = C_{I_1} - 20D/\epsilon$, and $y = C_{I_2} - 20D/\epsilon$ we have:

$$a^2 K_{I_3} + a(K_{I_3} x + K_{I_3} y - 1) + K_{I_3} xy = 0 \quad (4.10)$$

Equation (4.10) can easily be solved for a , and hence b and K_{T1} can be calculated. The ionic strength was essentially constant since all work was done in 0.01 M $HClO_4$. Therefore, the activity coefficient was calculated using an ionic strength of 0.01 in the Davies equation. These association constants with 95% confidence intervals are reported in Table X. The program used to calculate the association constant was set up such that any data point which gave a negative value was ignored.

The association constant was not calculated from Equation (2.18) because of some of the limitations mentioned by Woldbye (41). It was also noted that a small change in the value of Y_{max} could result in a large change in the calculated association constant.

The value of the enthalpy of the reaction at 25°C was found using Equation (3.10). A plot of $\log_{10} K_{T1}$ vs. $1/T$ for the $Tl(I_3)_2^-$ is shown in Figure 9. The value of ΔH° is $\Delta H^\circ = -9.12 \pm 0.25$ kcal/mole. The ΔG° and ΔS° values were -10.32 kcal/mole and $4 \pm .7$ e.u. respectively.

Spectral Data in CH_3CN

A similar study of both the KI_3 and TlI_3 systems was carried out in acetonitrile. The temperature range was limited to 5, 25, and 35°C, because of solvent evaporation problems and the spectra were recorded from 410 nm to 250 nm. At each temperature six ratios of the volume of I_3^- solution to total volume were used: .80, .75, .65, .55, .45, and .40. The spectra of KI_3 in acetonitrile were very similar to the water spectra. Table XI lists the absorption data for KI_3 at 25°C. The ace-

TABLE X

U.V.-VISIBLE DATA AT MAXIMUM ABSORPTION OF TlI_3 AT 45°C IN H_2O

$[\text{I}^-] \times 10^4$	$[\text{I}_2] \times 10^4$	$[\text{Tl}^+] \times 10^4$	v_i/v_t	Tabulated as Optical Densities			
				295 nm	360 nm	395 nm	370 nm*
8.02	1.61	0.40	.80	1.57	1.00	0.61	0.82
7.52	1.51	0.50	.75	1.41	0.88	0.53	0.76
7.02	1.41	0.60	.70	1.25	0.77	0.46	0.68
6.52	1.31	0.70	.65	1.08	0.66	0.39	0.60
6.02	1.21	0.80	.60	0.92	0.57	0.34	0.51
5.52	1.11	0.90	.55	0.76	0.48	0.28	0.44
5.02	1.01	1.00	.50	0.64	0.41	0.24	0.38
4.52	0.91	1.10	.45	0.52	0.33	0.19	0.32
4.02	0.81	1.20	.40	0.43	0.27	0.16	0.26

*The isosbestic point.

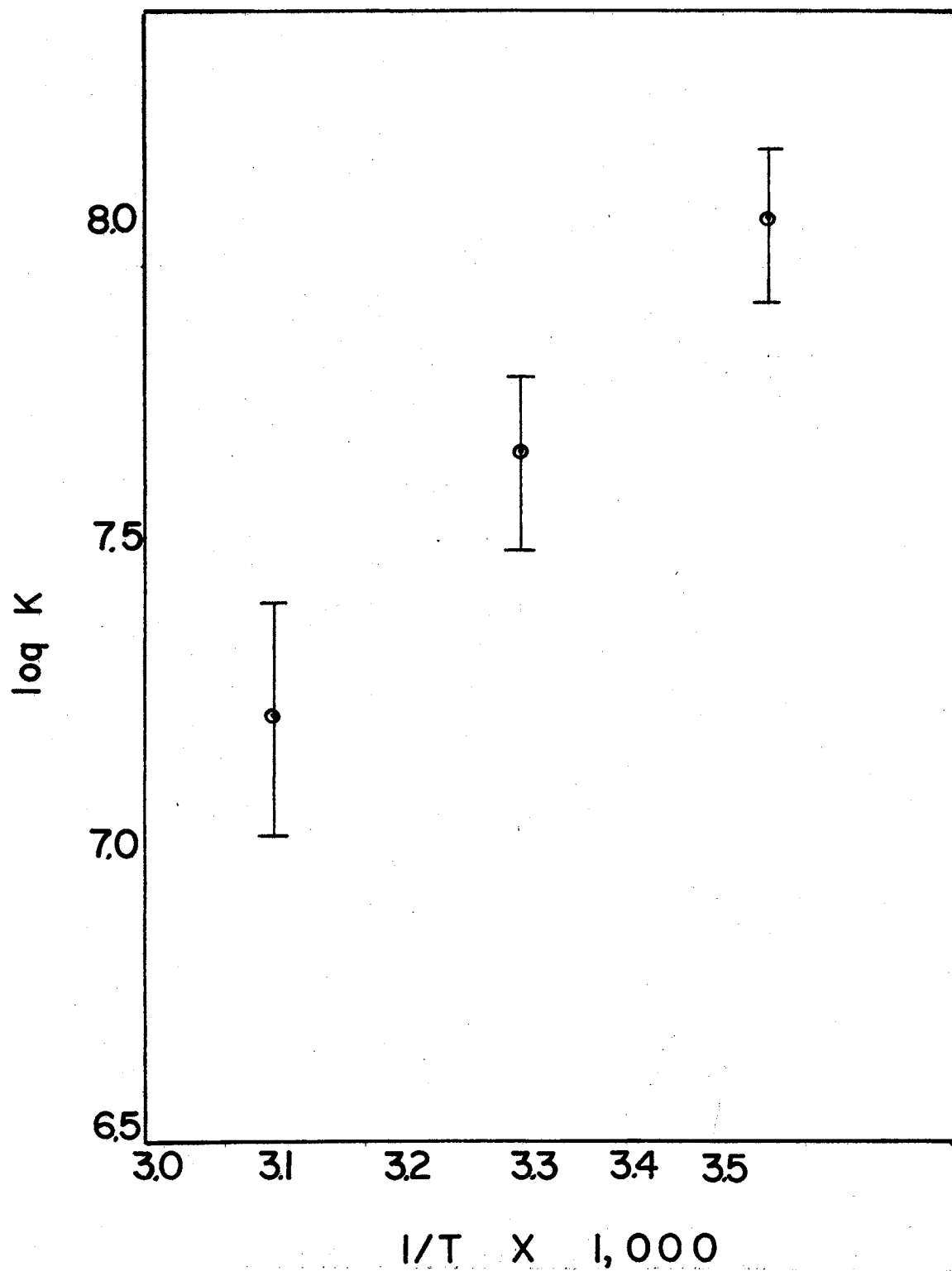


Figure 9. Plot of Log K vs. $1/T$ for $Tl(I_3)_2^-$ in H_2O

TABLE XI

ASSOCIATION CONSTANT OF $Tl^+ + 2I_3^- = Tl(I_3)_2^-$ IN 10^{-2} M AQUEOUS $HClO_4$

5°C	25°C	45°C
$(9.10 \pm 2.6) \times 10^7$	$(3.90 \pm 1.2) \times 10^7$	$(1.53 \pm .7) \times 10^7$

tonitrile data at 5 and 35°C show the same type trends with respect to 25°C as the water values. By plotting $(a-x)$ vs. $b(a-x)/OD$ the extinction coefficients and equilibrium constants for the formation of triiodide can be calculated. The extinction coefficients do not change significantly with temperature and have a value around 3.0×10^4 at 360 nm. Table XIII gives the equilibrium constants for the triiodide ion formation. Again no correction was made for any ion-pairing between potassium and triiodide at these low concentrations.

The enthalpy of formation of the triiodide ion at 25°C is calculated to be $\Delta H^\circ = -3.35$ kcal/mole and the standard deviation is probably somewhat larger than the water value. The entropy for the reaction is about 8.0 e.u.

The TlI_3 spectra were also recorded from 410 nm to 250 nm at 5, 25, 35°C. The same six ratios mentioned above were again used. However, instead of diluting each solution with the appropriate volume of solvent the solutions are diluted with a $TlClO_4$ solution. Again three different ratios of the stock concentration of Tl^+ to the stock concentration of I_3^- were used: 1:1, 1.5:1, and 2:1.

The results of the U.V.-visible study of the TlI_3 system were disappointing. The Job's plots gave a value of N , the number of bound ligands, equal to 1.5. Attempts were made to treat the data as a one to

TABLE XII

U.V.-VISIBLE DATA AT MAXIMUM ABSORPTION OF KI_3 AT 25°C IN CH_3CN

$[\text{I}^-] \times 10^4$	$[\text{I}_2] \times 10^5$	v_i/v_t	Tabulated as Optical Densities		
			295 nm	360 nm	395 nm
1.60	3.20	.80	0.95	0.48	0.28
1.51	3.02	.75	0.87	0.43	0.24
1.31	2.62	.65	0.79	0.40	0.18
1.11	2.22	.55	0.63	0.32	0.15
0.91	1.82	.45	0.41	0.21	0.09
0.81	1.62	.40	0.38	0.14	0.05

one complex and as a two to one complex, both of these methods gave negative association constants. If the system is treated as both a one to one and a two to one complex the number of unknowns exceeds the number of equations, hence, no solution is possible. The spectra do not show an isosbestic point.

TABLE XIII
EQUILIBRIUM CONSTANTS FOR I_3^- FORMATION IN CH_3CN

5°C	25°C	35°C
3.05×10^4	2.24×10^4	2.02×10^4

Work is still in progress on the matrix isolation of I_3^- ion. As of yet a satisfactory glass of water and I_2 has not been obtained.

CHAPTER V

KINETIC STUDY

Sutin et al. (57) have studied the kinetics of the triiodide ion formation using a laser Raman temperature-jump apparatus. The forward and reverse rate constants for this reaction are $(6.2 \pm 0.8) \times 10^9 \text{ M}^{-1} \text{ sec.}^{-1}$ and $(8.5 \pm 1.0) \times 10^6 \text{ sec.}^{-1}$ respectively. Since little data is available on the kinetics of Tl^+ complex formation it would be of interest to study the kinetics of formation of $\text{Tl}(\text{I}_3)_2^-$. It is expected that the reaction would be fast; hence, several relaxation techniques were attempted.

Several solutions of various concentrations were studied using the ultrasonic absorption apparatus available in this laboratory. No excess chemical absorption was observed even at very high concentrations. This is not surprising in light of the thermodynamics of $\text{Tl}(\text{I}_3)_2^-$ formation. The change in entropy for this reaction is small which by the Maxwell equation:

$$\left(\frac{\partial \Delta S}{\partial \Delta V}\right)_T = \left(\frac{\partial \Delta P}{\partial \Delta T}\right)_V \quad (5.1)$$

implies that the change in volume is also small. Since excess absorption is related to $(\Delta V)^2$ there should be little or no absorption of sound at ultrasonic frequencies. Indeed the same negative results were observed for I_3^- formation which was done at Sutin's request.

An attempt was also made to follow the reaction by a stopped flow technique. The reaction is apparently too fast for the stopped flow apparatus for which the dead time is about 5 milliseconds.

The reaction may be slow enough for study by conventional temperature jump techniques. Plans are also under way to study the reaction in cooperation with Professor E. M. Eyring, University of Utah, using the E-jump technique.

CHAPTER VI

DISCUSSION

Introduction

The objective of this work was to study cation-triiodide interaction to see if these interactions were of significance equal to if not greater than polyion formation. The cations chosen for this study were K^+ and Tl^+ . It was expected that experimental evidence for K^+ association would at best be marginal.

Raman Spectra

A study of $(CH_3)_4NI_3$ in water and KI_3 in formamide, which has a dielectric constant of 109, shows one strong band at 110 cm^{-1} . As was mentioned in Chapter II only a linear symmetric structure would give rise to this type of spectra. On the other hand, with a moderate ratio of KI/I_2 in water the Raman spectra shows a strong V_1 band at 110 cm^{-1} and a weak V_3 band at 145 cm^{-1} . These bands and their assignments are in agreement with those reported by Maki and Forneris (5). There are two structural models which can explain this spectra: a linear non symmetric molecule, and a non linear symmetric molecule. A study of the depolarization ratio supports the linear non symmetric molecule. Therefore, in solution it is feasible to conclude that the distortion from a linear symmetric molecule may be caused by solvent interaction or by ion-pair formation.

A rapid decrease of the V_3 band is observed on dilution of a mixture of $KI/I_2 = 1$ in water. However, the V_3 band is still distinguishable at concentrations ca. $10^{-3}M$. At this concentration it is reasonable to conclude that the triiodide ion distortion is solvent induced. As the dielectric constant of the medium is lowered the V_1 band becomes much sharper and a new feature is developed at 165 cm^{-1} . Both of these effects are consistent with a strong electrostatic interaction in a low dielectric medium. When the KI/I_2 ratio is increased to 3 in a low dielectric medium there is a moderate intensification of the 165 cm^{-1} band, and all three bands are distinctly separated. The assignment of the new band to a mode of the I_3^- ion is at best speculative, but it is tentatively attributed to the V_1 symmetric stretch being shifted towards the 218 cm^{-1} molecular I_2 value as association with K^+ lengthens the weaker I_3^- bond.

When the ratio of KI/I_2 in water is increased to 50:1 the intensity of the 165 cm^{-1} band increases very rapidly relative to that of V_1 . This data again supports the cation-anion interaction. The results of the LiI/I_2 study also support the conclusion of a cation-anion interaction.

When Tl^+ is used as the cation instead of K^+ a very dominant band develops. this band is due to a symmetric mode, depolarization ratio equal to 0.2, and from the U.V.-visible data it could be assumed to be due to the symmetric species $Tl(I_3)_2^-$. The fact that the asymmetric stretch remains active in the above system suggest that the 165 cm^{-1} band in high KI/I_2 ratios is the V_1 mode of a new species.

In summary, all of the Raman data suggest that there is an ion-pair formed in the $K^+ - I_3^-$ system. On the other hand, the Raman data in no way supports the formation of polyions, e.g., I_5^- and I_6^{-2} . The Raman

data definitely indicates an ion-pair formation in the $Tl^+ - I_3^-$ system. Hence, in general with a very large "soft" cation or in a high dielectric medium the triiodide ion is observed to be in a linear symmetric, $D_{\infty h}$, structure as evidenced by only one Raman band, V_1 . If the large "soft" cation is replaced by a smaller ion such as, K^+ or Li^+ a V_3 band becomes active. The cation-anion interaction is assumed to be end on with a lengthening of one of the triiodide ion bands. If the bonding in the complex is between a molecular orbital of the triiodide and the Tl^+ d-orbitals. The end on interaction is favored due the symmetry characteristics of the orbitals involved. Also, the orthogonal nature of the d-orbital will result in the highly directional bond that is indicated by the depolarization ratio. This effect is even more pronounced in a low dielectric solvent.

U.V.-Visible Spectra

The extinction coefficients and equilibrium constants calculated in the manner outlined in Chapter IV are in good agreement with those reported by Daniels (7), and other workers in the field (27,28), see Table XIV.

TABLE XIV

COMPARISON OF EQUILIBRIUM CONSTANTS OF I_3^- FORMATION AT 25°C IN H_2O

This Work	Ref. 7	Ref. 27	Ref. 28
760	723	768	748

No correction for ion-pairing was made, since at the concentrations used

($\sim 10^{-4}$ M) any ion-pairing would be small.

In the $Tl^+ - I_3^-$ system it was observed that the 360 nm band shifted to 395 nm as the Tl^+ concentration was increased. This is an indication of a new solute species. Further data analysis suggests that the species is a one to two complex which is significant to Raman interpretation.

The agreement of the thermodynamic values is somewhat poorer than the agreement for equilibrium constants as is seen in Table XV (8,11,27, 28).

TABLE XV

COMPARISON OF ΔG° , ΔH° , and ΔS° FOR I_3^- FORMATION AT 25°C, IN H_2O

	This Work	Ref. 8	Ref. 11	Ref. 27	Ref. 28
$\Delta G^{\circ*}$	-3.90	-3.88 ⁺	-3.50	-3.92 ⁺	-3.90
ΔH°	-3.80	-5.10	-3.10	-3.20	-4.05
ΔS°	0.30	-4.00 ⁺	1.40	2.00 ⁺	-0.49

* ΔH° and ΔG° are in kcal/mole and ΔS° is in e.u.

⁺ Calculated by author from reported values.

At this point it would be of interest to compare the thermodynamic properties of the $K^+ - I_3^-$ system in water and acetonitrile as well as the $Tl^+ - I_3^-$ system in water. Table XVI lists the thermodynamic properties of these three systems at 25°C. The most striking difference in the $K^+ - I_3^-$ system is the large increase in the entropy in the acetonitrile system. This change can be tentatively attributed to the differences in solvation of the iodine molecule in water and acetonitrile.

TABLE XVI
COMPARISON OF THERMODYNAMIC PROPERTIES

	K_1	ΔG° kcal/mole	ΔH° kcal/mole	ΔS° e.u.
$K^+ - I_3^-$ (H_2O)	760	-3.90	-3.80	~0
$K^+ - I_3^-$ (CH_3CN)	2.24×10^4	-5.92	-3.35	~8
$Tl^+ - I_3^-$ (H_2O)	$3.9 \times 10^{7*}$	-10.32	-9.12	~4

* Product of $K_1 K_2$.

Many people have tried to explain the discrepancies in the triiodine system by postulating the formation of polyions. For instance Ramette and Sandford (28) postulate the formation of the I_5^- polyion. Their method of approach was a solubility study with concentrations around 10^{-2} M in KI and 10^{-3} M in I_2 . At these concentrations our Raman studies indicate that an ion-pair is present and not a polyion. The above authors also reported values for ΔH° and ΔS° for the formation of I_5^- . These values are $\Delta H^\circ = +12$ kcal/mole and $\Delta S^\circ = +50$ e.u. which are a complete reversal of the trends seen for the triiodide formation. In a calorimetric study in this laboratory the reaction is exothermic. The experimental evidence for an I_5^- polyion is easily contestable and the discrepancies in the triiodide data it seems can be better explained on the basis of an ion-pair for which there is good experimental evidence.

The thermodynamic properties reported by Davies and Gwyne (27) for the formation of I_6^{2-} are believable in light of the thermodynamic

properties of the formation of the triiodide ion. The concentration range of their study was around 10^{-3} M, again it is pointed out that our Raman study indicates that an ion-pair is present at these concentrations. Theories of ionic interaction in solution point out that there is a small probability of an interaction between ions of similar charge type. The experimental method employed in this study was distributed between water and carbon tetrachloride, Bjerrum's theoretical model states a greater amount of ion-pairing is expected in the lower dielectric constant solvent. One would again expect that ion-pairs should be favored over I_6^{-2} in carbon tetrachloride.

In summary it is the conclusion of this work that the discrepancies in the interpretation of data on the triiodide ion should not be accounted for in terms of polyion formation but should be attributed to cation-anion interactions. Most of the work where polyions have been postulated have been done at high concentrations or in low dielectric solvents where ion-pairing would be expected. In the light of recent data on ion-pairing with K^+ this interpretation is not revolutionary. In support of our contention we offer the following explanation and interpretation. In the U.V.-visible study of the $Tl^+ - I_3^-$ system in water it was observed that as the Tl^+ concentration was increased with respect to the I_3^- concentration the 360 nm band shifts to 395 nm indicating some type of interaction and the formation of a new solute species. The depolarization ratio ($p = 0.2$) and the U.V.-visible interpretation are both consistent with a 2:1 stoichiometry for this new species. The interpretation of the Raman spectra of both cations is consistent with the existence of ion-pairs and most certainly at high concentrations of solute and solvents of low dielectric constant.

CHAPTER VII

SUGGESTIONS FOR FUTURE WORK

Since there is strong evidence for ion-pairing in the systems studied one suggestion for future work is to do an extensive thermodynamic study of other related systems using various experimental techniques, such as conductivity, calorimetry, and solubility. Once the thermodynamic properties are known a kinetic study can be made to get a complete picture of the system under study.

A specific project which pertains to the triiodide system should also prove to be interesting. This project would be to look at the Raman spectra of HI_3 in solution and isolated in a matrix. One possible way to obtain HI_3 in the matrix would be to carry out a high temperature gas phase reaction between H_2 and I_2 with a slight excess of I_2 . The reactants could then be trapped on a cold finger.

By isolating the triiodide ion in the matrix information can be obtained about the ion in the absence of any interference from a cation. This information would be useful in understanding the nature of the bonding of the triiodide ion with cations such as Tl^+ . The information from the matrix isolation would also help in understanding theoretical calculations.

A SELECTED BIBLIOGRAPHY

- (1) A. I. Popov, Halogen Chemistry, V. Gutmann, ed., Academic Press, New York, 1967, pp. 225.
- (2) Johnson, G. S., J. Chem. Soc., 31, 249 (1877).
- (3) Bancroft, W. D., Scherer, H. J. and Woolf, A. A., J. Chem. Soc., 2861 (1949).
- (4) Hayward, G. C. and Hendra, P. J., Spectrochem. Acta., 23, 2309 (1967).
- (5) Maki, A. G. and Forneris, R., *ibid*, 867 (1967).
- (6) Ginn, S. G. W. and Wood, J. L., Chem. Comm., 12, 262 (1965).
- (7) Daniels, G., Gazz. Chim. Ital., 90, 1068 (1960).
- (8) Awtrey, A. D. and Connick, R. E., J. Amer. Chem. Soc., 73, 1842 (1951).
- (9) Topol, L. E., Inorg. Chem., 10, 736 (1971).
- (10) Slater, J. C., Acta. Cryst., 12, 197 (1959).
- (11) Mironov, V. E. and Lastovkina, N. P., Russian J. Phy. Chem., 41, 991 (1967).
- (12) Katzin, L. I. and Gebert, E., J. Amer. Chem. Soc., 76, 2049 (1954).
- (13) Mooney, R. C. L., Acta. Cryst., 12, 187 (1959).
- (14) Tasman, H. A. and Boswijk, K. H., *ibid*, 8, 59 (1955).
- (15) Ehrlich, B. S. and Kaplan, M., J. Chem. Phys., 51, 603 (1969).
- (16) Sasane, A., Nakamura, D. and Kubo, M., J. Phys. Chem., 71, 3249 (1967).
- (17) Pimentel, G. C., J. Chem. Phys., 19, 446 (1951).
- (18) Person, W. B. et al., *ibid*, 35, 908 (1961).
- (19) Stammreich, H., Forneris, R. and Tavares, Y., Spectrochim. Acta., 17, 1173 (1961).

- (20) Brown, R. D. and Nunn, E. K., *Aust. J. Chem.*, 19, 1567 (1966).
- (21) Wiebenga, E. H. and Kracht, D., *Inorg. Chem.*, 5, 738 (1969).
- (22) Van Arkel, A. E. and De Boer, J. H., *Rec. Trav. Chim.*, 47, 593 (1928).
- (23) Wiebenga, E. H., Havinga, E. E. and Boswisk, K. H.,
- (24) Slater, J. C., *Acta. Cryst.*, 12, 197 (1959).
- (25) Herbo, C. and Sigalla, J., *Anal. Chem. Acta.*, 17, 199 (1957).
- (26) Awtrey, A. D. and Connick, R. E., *J. Amer. Chem. Soc.*, 73, 1842 (1951).
- (27) Davies, M. and Gwynne, E., *ibid*, 74, 2748 (1952).
- (28) Ramette, R. W. and Sandford, R. W., *ibid*, 87, 5001 (1965).
- (29) Devlin, J. P., et al., *Proc. XIV ICCS, Toronto, June 1972*.
- (30) Tobin, M. C., Laser Raman Spectroscopy, Wiley-Interscience, New York, 1971.
- (31) Raman, C. V., *Indian J. Phys.*, 2, 387 (1928).
- (32) Evans, J. C., Infra-Red Spectroscopy and Molecular Structure, M. Davies, ed., Elsevier Pub. Co., New York, 1963, pp. 199-205.
- (33) Heyde, M. E., et al., *J. Amer. Chem. Soc.*, 94, 5222 (1972).
- (34) Mortensen, O. S., *J. Mole. Spec.*, 39, 48 (1971).
- (35) Pimentel, G. C., *Spectrochim. Acta*, 12, 94 (1958).
- (36) Milligan, D. E. and Jarox, M. E., *J. Chem. Phys.*, 48, 2265 (1968).
- (37) Nancollas, G. H., Interactions in Electrolyte Solutions, Elsevier Pub. Co., New York, 1966, pp. 41-43.
- (38) Job, P., *Ann. Chim. (Paris)*, 9, 113 (1928).
- (39) Denison, R. B., *Trans. Faraday Soc.*, 8, 20 (1912).
- (40) Vosburgh, W. C. and Cooper, G. R., *J. Amer. Chem. Soc.*, 63, 437 (1941).
- (41) Robin, M. B., *J. Chem. Phys.*, 40, 3369 (1964).
- (42) Gabes, W. and Nijman-Meester, M. A. M., *Inorg. Chem.*, 12, 589 (1973).

- (43) Woldbye, F., *Acta. Chem. Sca.*, 9, 299 (1955).
- (44) Robinson, R. A. and Stokes, R. H. Electrolyte Solutions. Butterworth's Scientific Pub., London, 1959, pp. 1-24.
- (45) Bernal, J. D. and Fowler, R. H., *J. Chem. Phys.*, 1, 515 (1933).
- (46) Frank, H. S. and Wen, W. Y., *Dis. Faraday Soc.*, 24, 133 (1957).
- (47) Nemethy, G. and Scheraga, H. A., *J. Chem. Phys.*, 36, 3382 (1962).
- (48) Debye, P. and Hückel, E., *Physik, Z.*, 24, 305 (1923).
- (49) Davies, C. W., Ion Association, Butterworths, London, 1962, pp. 34-41.
- (50) Guggenheim, E. A., Thermodynamics, North Holland Publ. Co., Amsterdam, 1949.
- (51) Bjerrum, N., *Kgl. Danske Videnskab. Selskab, Mat. Fys. Medp.*, 7, 1 (1926).
- (52) Ritson, D. M. and Hasted, J. B., *J. Chem. Phys.*, 16, 11 (1948).
- (53) Wall, F. T., Chemical Thermodynamics, W. F. Freeman and Co., San Francisco, 1965.
- (54) Davies, W. G. and Prue, J. E., *Trans. Faraday Soc.*, 51.
- (55) Waters, D. N. and Basak, B., *J. Chem. Soc. (A)*, 2733 (1971).
- (56) White, W. D., Private Communication.
- (57) King, E. J., Acid-Base Equilibria, Pergamon Press, New York, 1965, pp. 194.
- (58) Sutin, N., et al., *J. Amer. Chem. Soc.*, 94, 1554 (1972).

VITA

John David Miller

Candidate for the Degree of

Doctor of Philosophy

Thesis: STRUCTURE AND THERMODYNAMICS OF METAL TRIIODIDES IN SOLUTION

Major Field: Chemistry

Biographical:

Personal Data: Born in Saint Louis, Missouri, October 15, 1945, the son of Mr. and Mrs. Opie J. Miller.

Education: Graduated from Theodore Roosevelt High School, St. Louis, Missouri, in June, 1964; received the Bachelor of Science degree in Chemistry, from Southeast Missouri State University, in June, 1968; received the Master of Science degree in Chemistry, Oklahoma State University in May, 1972, and completed the requirements for the Doctor of Philosophy degree in May, 1973.

Professional Experience: Taught freshman chemistry laboratories from September, 1967, to June, 1968, in the Department of Chemistry at Southeast Missouri State University; served as a teaching assistant from September, 1968, to May, 1973, at the Oklahoma State University.

Professional Organizations: American Chemical Society, Phi Lambda Upsilon honorary chemical society.